Universität Rostock Traditio et Innovatio

Master Thesis

Extraction of Physiological Data from Wearable Devices

Submitted by:

Manoj Sai Ghanta

Matrikel-Nr. 216100289

Submitted on:

Supervisors:

Prof. Dr.-Ing. Thomas Kirste

Dr. rer. nat. Sebastian Bader

UNIVERSITÄT ROSTOCK |Faculty of Informatics and Electrical Engineering |Institute of Visual and Analytic Computing |Chair of Mobile Multimedia Information Systems

Albert- Einstein Str.22, 18059 Rostock | Tel: +49 381 498 7511

Acknowledgements

I want to take this opportunity to thank Prof. Dr.-Ing. Thomas Kirste for allowing me to work on such an exciting topic for my master thesis. His team is fantastic and was very helpful throughout my thesis. I want to mention my special thanks to Dr. rer. nat. Sebastian Bader. I appreciate his concern and insights during my work. This project would not have been possible without his contributions and guidance. His patience is highly appreciated. I want to extend my gratitude to both.

I want to thank my friends for providing me with their support. I would also like to thank my parents for their support and encouragement. I will be in their debt forever. Above all, I am grateful to God for keeping me healthy and blessed.

Abstract

Generally, people aged above 65 years are much more prone to be affected by chronic disorders such as dementia, heart diseases and respiratory problems. In order to extend the life span and help them maintain a healthy lifestyle, chronic disorders have to be detected at an early stage of its onset. Due to the continuous growth of sensor technology, non-invasive methodologies have improved vastly; through these methods, the physiological parameters of the subjects can be monitored continuously.

In this work, two algorithms are developed to recover the pulse wave and respiratory wave from the raw data obtained from the PPG and accelerometer sensors, and by using those waves the Heart rate (HR) and Breathing rate (BR) features are estimated. The sleep recognition data collected using the wrist-worn sensors and Empatica E4 sensor data is collected from two subjects to estimate heart rate and breathing rate features. Further, the estimated features are cross-validated with the ground truth features obtained from the Electrocardiogram device. Moreover, to compare the estimated physiological features, the standard error metrics such as Root Mean Square Error (RMSE), Mean Absolute Error (MAE) and Correction Coefficient (CC) are evaluated using the ground truth features. From the results, the PPG heart rate estimation in both the datasets have better results compared to the accelerometer heart rate estimation.

Contents

List of Abbreviations v

List of Figures v

1 Introduction 1
1.1 Motivation . . . 2

2 Preliminaries 4
2.1 Cognitive impairments . . . 4
2.2 Wearable devices . . . 4
2.2.1 Motion sensors . . . 5
2.2.2 Photoplethysmography (PPG) . . . 6
2.3 Electrocardiogram (ECG) . . . 7
2.4 Signal Noise Reducing Filters . . . 8
2.4.1 Moving Average Filter . . . 9
2.4.2 Butterworth Filter . . . 9
2.5 Overview of Heart Rate Variability (HRV) . . . 11
2.5.1 Central Nervous System . . . 11
2.5.2 Heart Rate Variability (HRV) . . . 12
2.6 Evaluation Metrics . . . 12
2.6.1 Mean Absolute Error (MAE) . . . 13
2.6.2 Root Mean Square Error (RMSE) . . . 13
2.6.3 Pearson Correlation Coefficient . . . 14

3 Literature Review 15
3.1 Search queries and Search engines . . . 15
3.2 Important terminology . . . 17
3.3 State of the Art . . . 18

4 Data preprocessing and features extraction 26
4.1 Data acquisition . . . 26
4.1.1 Sleep recognition data . . . 26
4.1.2 Experimental Dataset . . . 26

4.2 Signal Preprocessing 27
4.2.1 Estimation of Pulse Wave 28
4.2.2 Estimation of Respiratory Wave 30

5 Heart Rate and Breathing Rate Estimation **31**
5.1 Pulse Wave Peak Detection 31
5.1.1 Time-domain analysis 32
5.2 Breathing Rate Estimation 33
5.2.1 Frequency-domain analysis 34
5.2.2 Breathing rate (BR) feature 34

6 Results and Discussions **36**

7 Conclusion and Future work **45**

Bibliography **I**

List of Figures

2.1 The six independent variables describing the motion characteristics of an motion sensors. [1] 5
2.2 Graphical representation of sinusoidal wave from a PPG sensor due to change in blood volume [2] 7
2.3 Operating principle of transmitive and reflective for PPG sensor [3] 7
2.4 Normal features of the ECG wave [4]. 8
2.5 Low pass filter [5] 10
2.6 High pass filter [5] 10
2.7 Butterworth band-pass filter [4] 11
2.8 The graphical representation of mean absolute error (MAE). 13
2.9 Graphical plots show Pearson correlation coefficient relations: (a) represents positive correlation, (b) represents negative correlation, (c_1 and c_2) indicates absence of correlation [6] 14

3.1 The flowchart explains the process followed to study and gradually filter the important research papers. 15

4.1 The flowchart provides overview of PPG raw data-preprocessing processor till extraction of pulse wave and respiratory wave. 27
4.2 An example of raw PPG wave and pulse wave comparison plot 29
4.3 The flowchart explains the data preprocessing procedure of 3-axis accelerometer till extraction of pulse wave and respiratory wave 29
4.4 An example of raw accelerometer wave and respiratory wave comparison. . . 30

5.1 Figure shows QRS complex of PPG wave. 31
5.2 The flow chart provides overview of how Heart rate and Breathing rate features are extracted. 32
5.3 Figure representing varying time-series frequency between (R-R intervals) and adjacent (R-R intervals) 33
5.4 Frequency spectrum of Heart Rate Variability [7] 34

6.1 The plot shows the comparison of estimated and ground truth heart rate feature for sleep recognition PPG sensor data set, for subject-1. 37

6.2 The plot shows the comparison of estimated and ground truth heart rate feature for sleep recognition PPG data set, for subject subject-2. 37
6.3 The plot shows the comparison of estimated and ground truth heart rate feature for sleep recognition 3-axis accelerometer data set, for subject-1. . . . 38
6.4 The plot shows the comparison of estimated and ground truth heart rate feature for sleep recognition 3-axis accelerometer data set, for subject-2. . . . 38
6.5 The plot shows the comparison of estimated and ground truth heart rate feature for Empatica E4 PPG data set, for subject-1. 40
6.6 The plot shows the comparison of estimated and ground truth IBI feature for Empatica E4 PPG data set, for subject-1. 40
6.7 The plot shows the comparison of estimated and ground truth heart rate feature for Empatica E4 PPG data set, for subject-2. 41
6.8 The plot shows the comparison of estimated and ground truth IBI feature for Empatica E4 PPG data set, for subject-2. 41
6.9 The plot shows the comparison of estimated and ground truth Breathing rate feature for sleep recognition accelerometer data set, for subject-1. 42
6.10 The plot shows the comparison of estimated and ground truth Breathing rate feature for sleep recognition accelerometer data set, for subject-1. 43
6.11 The plot shows estimated breathing rate parameters, extracted from E4 PPG data set, for subject-1. 43
6.12 The plot shows estimated breathing rate parameters, extracted from E4 PPG data set, for subject-2 44
6.13 The plot shows estimated breathing rate parameters, extracted from E4 accelerometer data set, for subject-1. 44
6.14 The plot shows estimated breathing rate parameters, extracted from E4 accelerometer data set, for subject-2. 44

1 Introduction

According to research, people aged above 65 years are more prone to chronic disorders such as Dementia. Dementia can cause several cognitive impairments, such as :

1. Memory loss.
2. Loss of decision-making skills.
3. Repetition of the same task.
4. Misplacing things.
5. Inability to recognize familiar people and places.
6. Frequent changes in emotional gestures. [8] [9]

A recent forecast by the US Census Bureau predicts that by 2050, more than 100 million people will be affected with dementia out of which 14 million will be Europeans [10]. In the United States, approximately 5.4 million people are affected by dementia. Out of the 5.4 million people, 5.2 million dementia patients are aged over 65 years. Therefore, this number will only increase as the percentage of older adults increases. According to health organisations, dementia in older adults is one of the biggest global public health and social care challenges [9]. Earlier, clinical and diagnostic tests were utilised in identifying cognitive impairments in dementia patients, but, those identification studies have failed in more than 50% of the cases. Reports indicate that family members were able to recognise primary or mild dementia complications but not general healthcare facilities [11].

In the last few decades, many studies proposed methods for early detection and automatic disease prediction with higher accuracies using advanced body-worn inertial sensors and bio-sensing technologies such as accelerometer, gyroscope, magnetometer, pressure sensor and heart rate sensors such as photoplethysmogram (PPG), electrocardiogram (ECG). These sensors are feasible not only to access outward gestures of patients but also accessible to inward physiological patterns of Central Nervous System (CNS). In daily life, there is significant variation in activity patterns when compared to laboratory studies. Therefore, an estimation of cognitive impairments based on wearable sensors is still challenging [12].

In this research, we rely on data obtained from wearable devices (smart watches) which have a multitude of sensors such as:

1. 3-axis accelerometer.
2. 3-axis gyroscopes.
3. Heart rate sensor.

The aim of this work is to research statistical methods as well as machine learning algorithms to derive high-level physiological features from the data obtained from multiple sensors. In this work, an available data set which includes the raw sensor data collected by a wrist-worn sensor and medical data from patients is used as the ground truth. The pre-processing of wrist-worn data is done using average filters and Butterworth band-pass filters with cut-off frequencies to reduce noise in the signal. Based on the ranges of filters, the pulse wave and respiratory wave are computed [13]. Further, the magnitude is calculated from the 3-axis accelerometer and 3-axis gyroscope signal. This magnitude data is segmented to particular window size, and later the peaks are enhanced from the segmented data. Then by collecting the peak list and peaks difference from the segmented data and the time domain and frequency domain analysis, Heart Rate variability (HRV) and Breathing Rate (BR) features are extracted in frequency analysis [14]. The PPG and ECG sensors have the same pre-processing procedure of motion sensors. At the estimation phase, the features from the wrist-worn sensor are compared with ground truth ECG featured vectors with the standard error calculation metrics such as root-mean-square-error (RMSE), normalised RMSE (nRMSE), and the mean-absolute-error (MAE). If error per cent is less than the standard research thresholds, then it indicates the wrist-worn sensors are feasible with the golden standard, i.e., ECG device.

1.1 Motivation

At present, the global health care organisations are worried about the growth of the adult population. According to researchers, people aged above 65 years are affected by chronic disorders such as dementia, cardiac attacks, respiratory health problems [14]. In order to control these health issues in adults, several traditional invasive methods are implemented based on cortisol level in the past. Further, non-invasive methodologies are implemented to improve the quality of healthcare and reduces the cost of first healthcare detections measures. These predictive devices are tightly coupled with the advancement of electronics for, e.g., Electrocardiography (ECG) which is considered as the golden standard device for estimation of cardiac and breathing rates and physiological parameters [15]. In contrast, there are some issues with the device. The ECG consists of two capacitive chargeable electrodes that are attached to the skin, and a liquid gel is applied to increase the strength of the signal but this set up may lead to skin infections, signal deterioration, and while monitoring daily physiological life activities for more extended period of time, it might obstruct the routine of the person and disrupt the daily life [16]. However, to overcome this current state-of-problem, different research teams have

developed several unobtrusive wearable sensing devices such as wrist-worn sensor (watch type) [16], this device is integrated with 3D accelerometer, 3D gyroscope, Photoplethysmography (PPG) sensors, clip-free eyeglasses device for monitoring heart rate, h-shirt for measuring heart rate and blood pressure [17], and glove based photonic textiles as wearable pulse oximetry [17]. The rapid growth of integrated circuit technologies and microelectromechanical technologies (MEMS) has led to a drastic change in the size of signal processing bio-potential electrodes and inertial measuring units (IMU) [18].

The motive of this thesis is to use wrist-worn device data and extract heart rates and breathing rates physiological features, and further validate this extracted feature vectors with ground truth ECG features by implementing error calculation methods. If the errors values are less when compared with standard threshold data, the Electronic device ECG can be replaced with mobilised wrist-worn sensors device. These devices can continuously monitor patients health at any instant time in 24 hours with comfort and even reduces experimental signal processing artefacts.

2 Preliminaries

2.1 Cognitive impairments

Cognitive impairments are not based on disease and are not limited to a particular age group, but most of the research surveys show that people aged above 65 years are effected with these impairments. The cognitive impairments have different stages, at a mild stage the people can make their daily life activities, but the severe level of cognitive impairments can cause dementia, Alzheimer's diseases, cardiovascular diseases and respiratory problems. Till now, there is no complete medication to cure these health problems, but early detection of these diseases can save and improve people's lifestyle. These are a few common symptoms of cognitive impairments [19] [20].

1. Memory loss.
2. They are not capable of making their own decisions.
3. Repeating the same conversations.
4. Frequent mood swings.
5. Vision deficiency and cannot recognize familiar people and places.

In the past, few traditional invasive detection methods are implemented to predict cognitive impairments, with the advancement in electronics, an Electrocardiogram (ECG) device which can extract physiological information from subjects is used now. From the last decade, ECG standard devices are being replaced with wrist-worn wearable sensors to detect cognitive impairments at early stages [20].

2.2 Wearable devices

In recent years, there is a development of micro-electronic-mechanical-systems technology towards wearable computing devices. These devices have communication capabilities, continuous power supply within a small instrument, and it costs less as well. The wearable wrist-worn sensor such as (Empatica E4) consists of 3-axis accelerometer, 3-axis gyroscope, 3-axis magnetometer and Photoplethysmography (PPG) [21], can continuously monitor physiological parameters such as Heart Rate Variability (HRV), Breathing

Rate (BR) and invasive blood pressure. These features help in predicting chronic disorders with high accuracies, and they can also be applied in the rehabilitation. In the below sub-sections, the basic working principles of wrist-worn sensors is explained [2].

2.2.1 Motion sensors

The motion sensors or inertial sensors play an essential role in human health care, for example, the head rotation and body gestures are the input signal for human body balance, they identify chest wall movements to precisely monitor breathing rate, and these sensors also used in rehabilitation programmes to closely monitor people with disabilities. General motion artefacts of a human body, an organ or tissue can be illustrated by six independent variables. Therefore, to precisely measure motion characteristics, six degrees of freedom sensing capability is required. Figure 2.1 shows three linear motion along the axis: sway, heave and surge and three angular movements perpendicular to the axis: roll, pitch and yaw. For instance, the human vestibular system is a sensible and sophisticated organ located in the ear that can accurately detect six independent variables and these variables are interpreted by the central nervous system (CNS) to make human body stable [1].

In practical engineering applications, the linear and angular motions are detected by using accelerometer and gyroscope respectively. An accelerometer is an inertial device which can measure acceleration with respect to gravity along each axis. The operating principle of an accelerometer is based on mechanical sensing, it has a proof mass attached to the spring and a damper, with respect to a cantilever beam. The displacement of the proof mass is due to the inertial force, which can deflect the beam and derive linear acceleration along each axis. On the other hand, gyroscope consists of two sets of mass-spring-damper-beam mechanisms, one for driving and the other one is for sensing body motions and gestures using the angular rates [1] [22].

2.2.2 Photoplethysmography (PPG)

Photoplethysmography (PPG) sensor also known as Blood Volume Pulse (BVP) sensor, is a wearable bio-medical device with optical capabilities, it follows a non-invasive technique that measures the dynamic change in blood volume at each instant of time from the skin tissues (fingertips, earlobes, forehead, wrist). Figure 2.2 shows a graphical representation of the sinusoidal wave pattern, where the pattern replicates the cardiac cycle with systole and diastole phases. The systole phase implies the heart contraction with the inflow of blood into the arteries, during the diastole or restoring phase blood passes through the veins [3] [23].

Usually, a PPG sensor signal consists of a pulsating Alternating Current (AC) component and a non-pulsating Direct Current (DC) component. The AC component has a form similar to a cardiac cycle due to sequential relativity of light due to the change in blood volume expelled through the arteries. Later, this sinusoidal wave pattern is

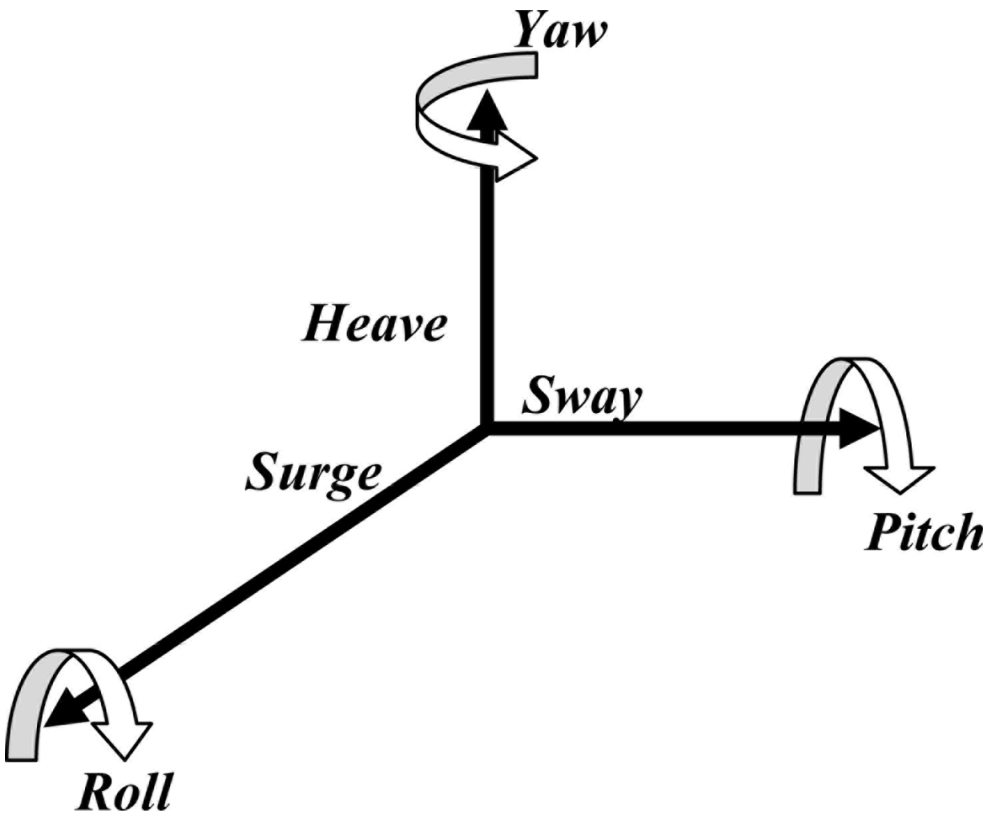

Figure 2.1: The six independent variables describing the motion characteristics of an motion sensors. [1]

passed into the Photo Detector (PD) that reduces the unwanted noise using filters and converters to maintain positive co-relations with the amount of blood that reaches the tissues. The Direct Current (DC) component based on the observance factor, which is related to the features on the skin tissues. The DC signal is neglected using low-pass filters mounted in sensor [3] [24].

The PPG sensor is divided into two modes considering the functionality principles shown in Figure 2.3, that is transmission or reflection of light on specific parts of the human body. The transmission type as shown in Figure 2.3, where the LED light is transmitted into the index finger, the output light frequencies or signal frequencies periodically vary in correspondence to the change in blood volume. Then, this signal passes to the Photo Detector (PD) to quantify it by using the sensor mechanism, Figure 2.3 shows that the LED light and Photo Detector (PD) are located opposite to each other. In the reflection type sensor , the LED light is focussed onto the skin and further this incident light is reflected onto the Photo Detector (PD) because both LED light and the Photo Detector (PD) are placed adjacent to each other.

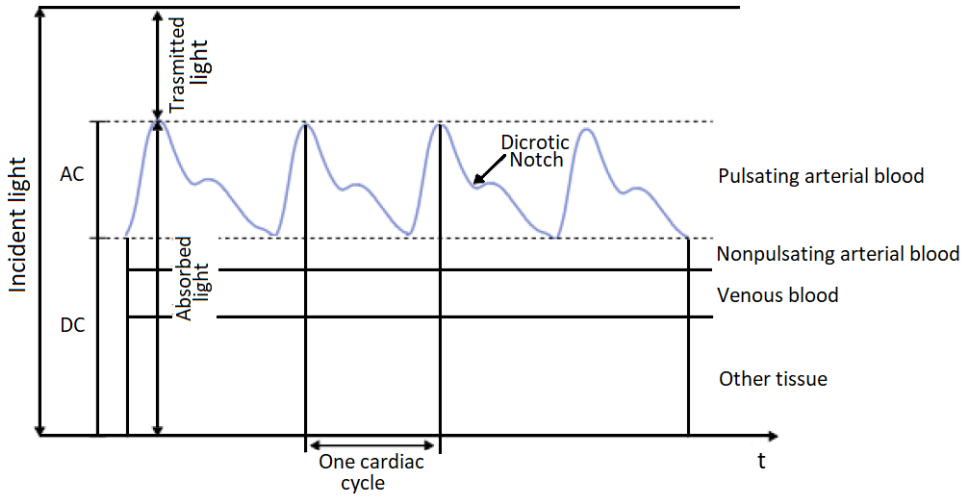

Figure 2.2: Graphical representation of sinusoidal wave from a PPG sensor due to change in blood volume [2]

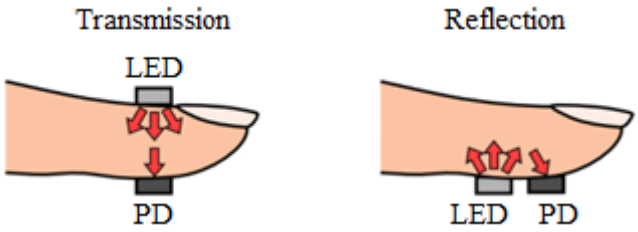

Figure 2.3: Operating principle of transmitive and reflective for PPG sensor [3]

Therefore, this PPG sensor signal is widely used to predict cardiovascular diseases at early stages by calculating measurable features like Heart Rate Variability (HRV) and Blood Pressure (BP) [24] [7].

2.3 Electrocardiogram (ECG)

An Electrocardiogram (ECG) is a cartesian representation of the potential difference generated at the surface of the chest during the electrical activity of the heart. The ECG is carried out by varying the number of electrodes between three and twelve, and a liquid gel is used to avoid the presence of air. The ECG is invented in 1887, from then on, it is an invaluable diagnostic device which can capture heart abnormalities at early stages and helps in increasing the lifespan [25].

Willem Einthoven received a noble prize for his discovery of the ECG mechanism in the year 1924 in the field of physiology [26]. Figure 2.4 represents a pattern of ECG

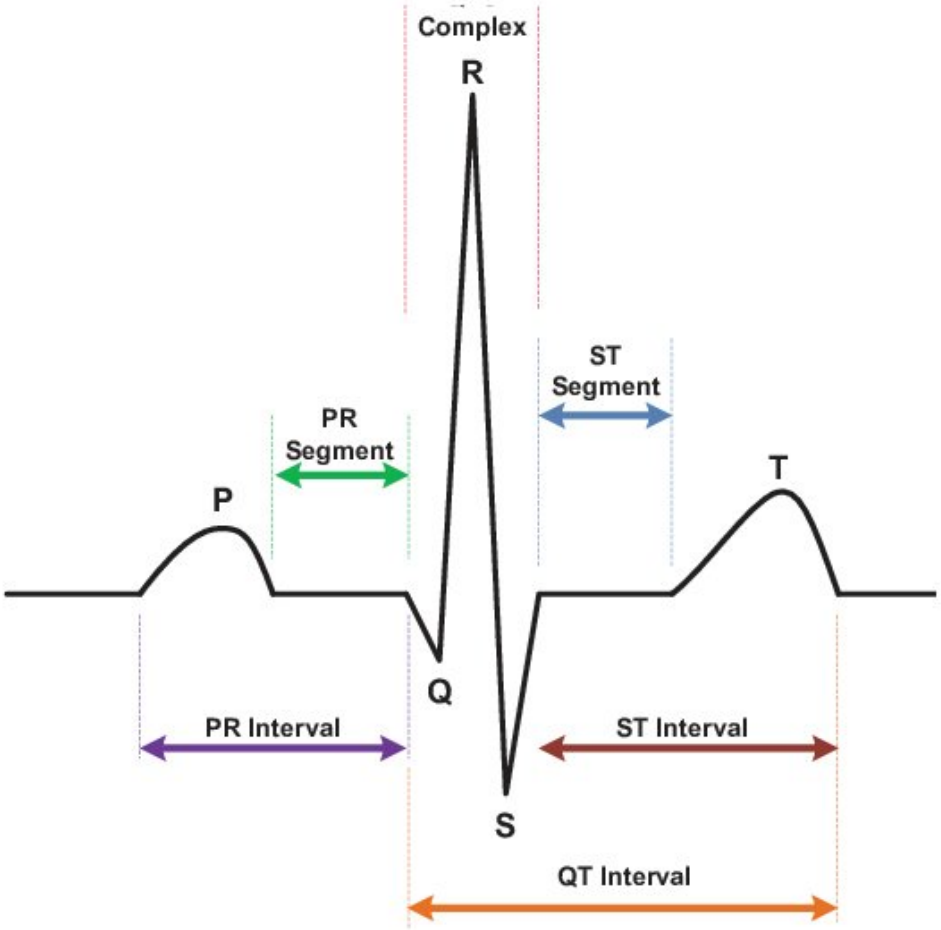

Figure 2.4: Normal features of the ECG wave [4].

signal with p-wave, QRS complex wave and the T-wave for a heart at standard condition. Each of this wave appears due to the electrical potential difference of the heart rate. The ECG signal is divided into the depolarization phase and re-polarization phase. The p-wave and QRS complex wave correspond to the depolarization phase of the heart rate signal, the T-wave represents the re-polarization phase of the heart rate signal. The ECG signal has wave patterns that are similar throughout the signal path [4].

2.4 Signal Noise Reducing Filters

Generally, the raw time series signal from a wearable sensor has non-isolated frequencies, signal shifts and trends due to body motion during experimental tasks. In order to remove this noise artefacts from the data, data pre-processing digital filters such as Mov-

ing averaging filters, Butterworth band pass filters, Adaptive band pass filters, Kalman Filters and Fast Fourier Transformation are applied [27]. In the below subsections the basic theory and working principals of noise reducing filters utilised in this work are explained.

2.4.1 Moving Average Filter

The moving average can be applied to one or more time-series sequences to remove random noise while maintaining sharp timestep response on the signal. As the time series signal consists of small variations between time shifts and trends, the window size should be mentioned to calculate moving average value. The moving average value or filter value is calculated by the sum of a symmetric window along with the data. The obtained dataset is used as an input for time predicting algorithms [28]. The mathematical equation of moving average is shown in the below equation 2.1. In the below equation x[i+j] is an input time signal, the index j is limited from 0 to N-1 which corresponds to change in summation, and y[i] is an output signal [29].

$$y[i] = \frac{1}{N} \sum_{j=0}^{N} -1x[i+j] \tag{2.1}$$

Generally, two types of moving average filters are used such as centered and trailing moving average. But trailing moving average is mostly used for data pre-processing [28].

2.4.2 Butterworth Filter

Filters act as networks that pre-process the signal in a frequency-dependent domain. Generally, filters are classified based on the signal nature such as low-pass filter, high-pass filter, band-pass filter and stopband. These filters are utilised in many practical applications. The low-pass filter is applied to stabilise the signal by rolling off high frequencies, where excessive frequency shifts may lead to unwanted oscillations, and the high-pass filters are used to block dc offset (mean amplitude of the signal) in high gain frequencies. Moreover, this filter is used to divide signals in the region of interest (ROI) and removes random trends in the data [5].

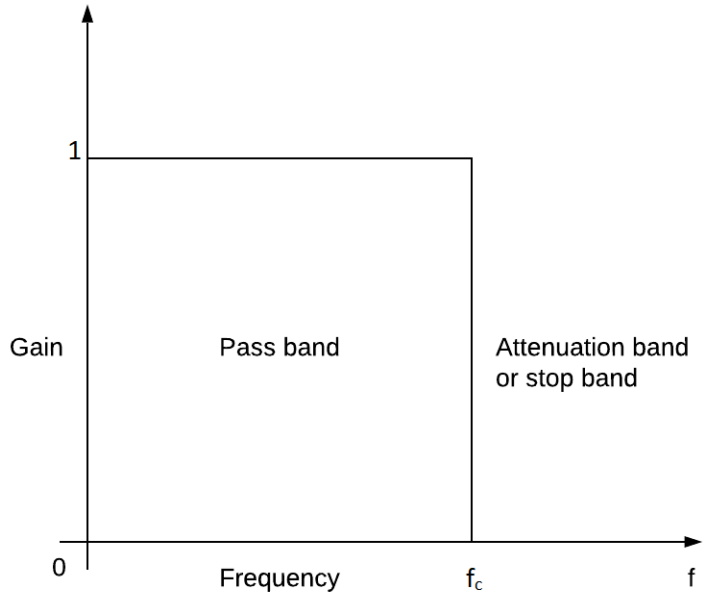

Figure 2.5: Low pass filter [5]

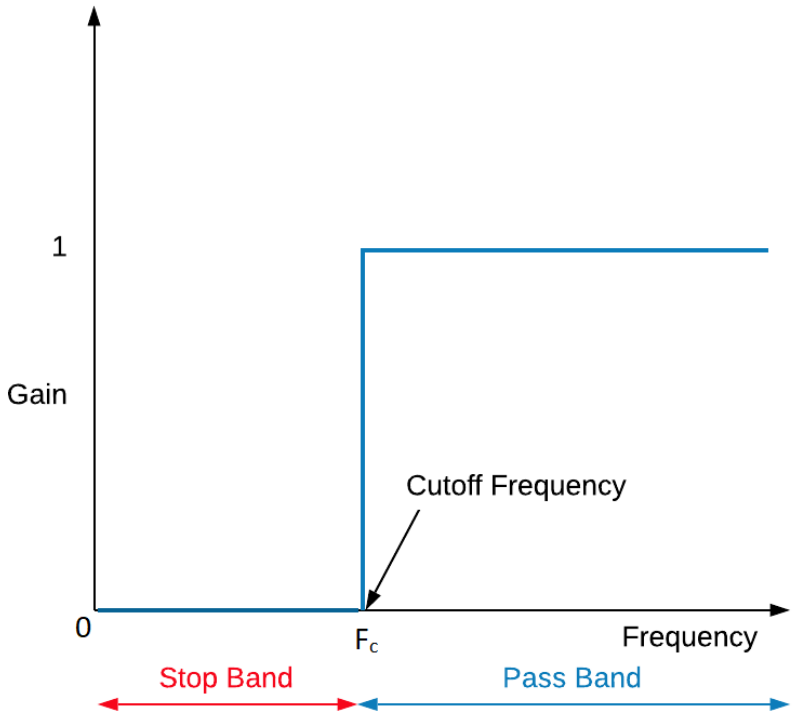

Figure 2.6: High pass filter [5]

The bandpass filter allows the signal to pass only if the frequency is in between two specific frequencies and sets every other response to zero, this is called as stopband. If a frequency response varies from passband to stopband, this is known as cut-off frequency. Figure 2.5 indicates normalized low pass filter, which has higher frequencies in stopband and low frequencies in the passband, the filtering principle of the high-pass filter is vice versa to the low-pass filters [5] as shown in the Figure 2.6.

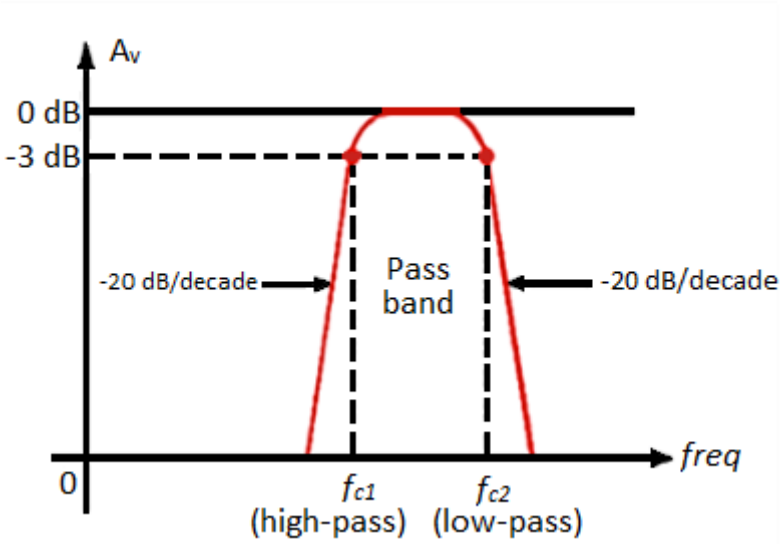

Figure 2.7: Butterworth band-pass filter [4]

The band-pass filter (BPF) with a limit of -3 decibel (dB)/decade is known as Butterworth filter. This filter insists the signal to stay in between low and high critical frequency limits and other frequencies around them are rolled off to zero with differential orders such as first order, second order, third order, by altering order rate. The steepness of the signal curve is varied, and this curvature change reflects the change of the roll-off value of the stopband. For example, in Figure 2.8, based on the given order, the roll-off is -20dB/decade in the stopband. The f_{c1} and f_{c2} are high and low cut-off frequencies for band-pass Butterworth filter [4].

2.5 Overview of Heart Rate Variability (HRV)

2.5.1 Central Nervous System

We know that the Autonomous Nervous System (ANS) regulates various internal organs of the human body. The nervous system is also known as the Central Nervous system (CNS) or involuntary motor system. Again, the ANS is subdivided into sympathetic and parasympathetic nervous systems. The sympathetic nervous system corresponds to

the ”fight or flight” mechanism. Therefore, this mechanism tends to increase the action potential or electrical stimulation at the sinoatrial node, which leads to increased Heart Rate (HR). The heart is forced to contract within the depolarisation phase [7], in this phase, the human body consumes more amount of energy due to the increase of cardiac muscle strength, during this mechanism the working of the digestive system kept low [30].

The parasympathetic nervous system represents the ”rest or digest” mechanism, which follows re-polarisation or restoring phase. In this phase, there is a decrease in heart rate and blood pressure, thereby increasing the functionality of the digestive system. From the above text, we can notice that both sympathetic and parasympathetic systems perform different actions, the Autonomous Nervous system (ANS) balances the nervous systems using feedback mechanisms, this balanced phenomenon is known as sympathovagal balance [31] [7] [32].

2.5.2 Heart Rate Variability (HRV)

In the 18th century, Stephen Hals observed variations in arterial blood pressure during the respiration cycle. Later, Carl Ludwig illustrated the relationship between heartbeat fluctuations and respiratory sinus rhythms [23]. In 1965, Hon and Lee noticed that the variability in stress levels are due to beat-to-beat or RR intervals variations. During 1970’s Ewing et al. applied signal processing measures on RR intervals to predict Autonomous Nervous System behaviour in diabetic patients. In 1966, a big move was taken by the European Society of Cardiology and North American Society of Pacing and Electrophysiology. These societies hired researchers from various fields like Data analysts, mathematicians, psychologists, biologists to find standardised nomenclature for Heart Rate Variability signal [33] [34].

The Heart Rate Variability (HRV) describes a series of sequential time variable frequencies between consecutive heartbeats. It also measures the variations between consecutive heart rates. In the last four decades, researchers focused on the relationship between the ANS system and cardiovascular rhythms. The ANS nervous system modulates the heartbeat by using the SA node (primary pacemaker of the heart). The heart rate varies quickly under the influence of the sympathetic nervous system, and on the other hand, the heart rate decreases under the parasympathetic nervous system. The two systems are activated based on the sympathovagal balance.

2.6 Evaluation Metrics

In this work, to evaluate estimated output features with the original or ground truth features, we have implemented few statical linear regression metrics such as Mean Absolute Error (MAE), Root Mean Square Error (RMSE) and Correction Coefficient (CC). Each error metrics calculate the difference between the ground truth value and model

output value to predict residuals. Finally, the obtained residuals values are condensed to a single output residual, and this estimated value judges the ability of our model.

2.6.1 Mean Absolute Error (MAE)

The Mean Absolute Error (MAE) is a linear regression metrics, which takes only the absolute difference between each actual output value and predicted output value to calculate residual or error. However, each residual value is linearly contributed to estimate the total amount of error value. If the total error value of MAE is small, then it tells us that the model is capable. On the other hand, if the error value is high, then it suggests that there are some issues in the modelled algorithm or the obtained dataset [35]. In the MAE formula, the variable 'n' represents the total number of data points, y_j and $\hat{y}_j$ corresponds to actual output value and the predicted output value for the interval (j=1,2,3..,n).

$$MAE = \frac{1}{n}\sum_{j=1}^{n}|y_j - \hat{y}_j| \tag{2.2}$$

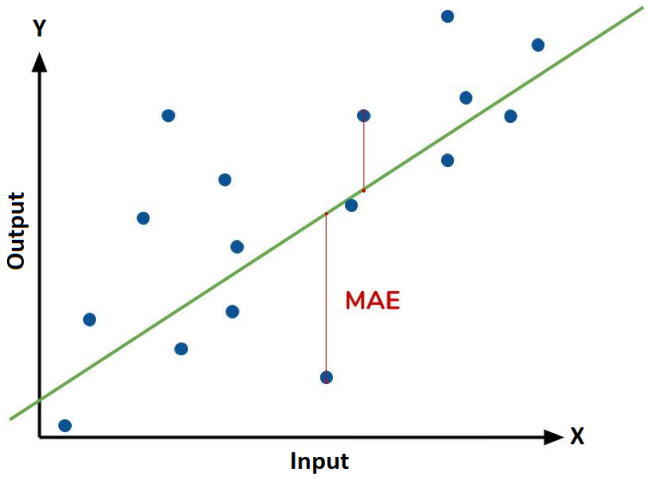

Figure 2.8: The graphical representation of mean absolute error (MAE).

Figure 2.8 is the graphical representation of mean absolute error (MAE). The blue points represent the data points, and the linear green line represents the model predictions, the red line indicates the Mean absolute error.

2.6.2 Root Mean Square Error (RMSE)

The working principle of the Root Mean Square Error (RMSE) metric is similar to MAE error. It measures the average magnitude of the errors to predict the model ability.

However, the difference is instead of taking absolute values it squares the residuals and averages the squares for the 'n' number of data points, and the square root is calculated. The y_j and $\hat{y_j}$ indicates the actual value and predicted value for the interval (j=1,2,3..,n) [35].

$$RMSE = \sqrt{\frac{1}{n}\Sigma_{j=1}^{n}\left(\frac{y_j - \hat{y_j}}{n}\right)^2} \tag{2.3}$$

2.6.3 Pearson Correlation Coefficient

The Pearson Correlation Coefficient (CC) is a widely used formula in statistics and it was proposed in 1896 by Pearson. It is also known as linear or product-moment correlation coefficient; it estimates the linear relationship value 'r' between actual and predicted datasets. The CC value does not rely on the specific measurements units. The correlation coefficient value varies between -1 and +1. It indicates the exact linear relationship between the two datasets. If the correlation coefficient is zero, it implies no correlation. The negative CC values indicate the increase in predicted values and a decrease in actual value. On the other hand, the positive correlation values imply the increase in both the predicted value and the actual value [6].

$$CC = \frac{N\sum_{i,j=1}^{N} X_i Y_j - (\sum_{i=1}^{N} X_i \sum_{j=1}^{N} Y_j)}{\sqrt{[N\sum_{i=1}^{N} X_i^2 - (\sum_{i=1}^{N} X_i)^2][N\sum_{j=1}^{N} Y_j^2 - (\sum_{j=1}^{N} Y_j)^2]}} \tag{2.4}$$

In equation 2.4 , The value 'N' indicates the number of sample points, X and Y values correspond to actual values and predicted values.

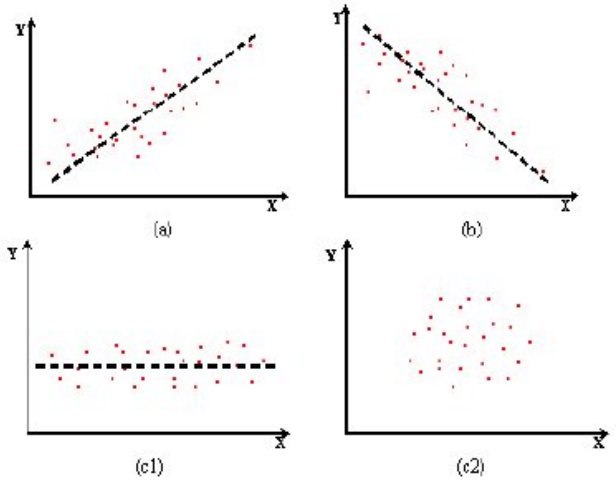

Figure 2.9: Graphical plots show Pearson correlation coefficient relations: (a) represents positive correlation, (b) represents negative correlation, (c_1 and c_2) indicates absence of correlation [6]

3 Literature Review

There are several studies performed around the world on the topic of extracting physiological features using non-invasive medical devices equipped with sensors. The extracted features are then compared with the ground truth using statistical and machine-learning methods. These papers are studied and summarised below.

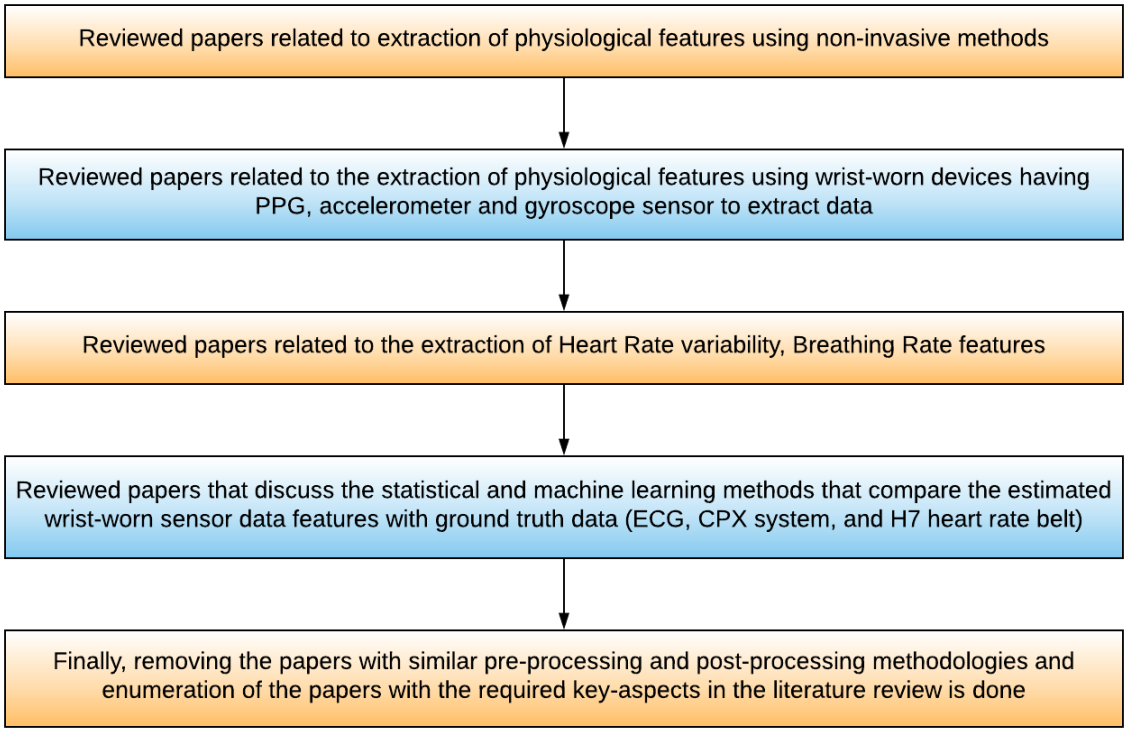

Figure 3.1: The flowchart explains the process followed to study and gradually filter the important research papers.

3.1 Search queries and Search engines

The search queries used for literature review:

1. Heart rate variability and Breathing rate.

2. How to extract physiological features from accelerometer and gyroscope.
3. Extraction of heart rate variability and breathing rate features from dementia patients with wearable sensors.
4. Estimation of HRV and breathing rate from adults using the PPG sensor.
5. How to extract statistical features from mobile wrist-worn sensors.
6. Statistical and machine learning algorithms to estimate HRV and breathing features.
7. Algorithms to cross-validate wearable sensors data features with ECG data features.

The search engines used :

1. Google scholar
2. IEEE
3. PubMed
4. dblp
5. Europe PMC

3.2 Important terminology

The below table illustrates the important terminology based on research papers methodologies.

Table 3.1: Import terminology from research papers.

Processing phases	Important Terminology
Chronic disorders	Cognitive impairments, dementia, Alzheimer's diseases, cardiovascular diseases and respiratory problems.
Types of wearable sensors used	3-axis accelerometer, 3-axis gyroscope, Photoplethysmography (PPG), Electrodermal Activity (EDA), Electrocardiography (ECG), Samsung Galaxy Gear watch, Empatica E4 wristwatch, Polar H7 heart rate belt.
Signal preprocessing	Data normalization, segmentation, Moving average filter (MAF), Butter-worth band-pass filter, adaptive band-pass filters, Kalman filters, Chebyshev filters, FIR band-pass filter, Discrete Wavelet Transformation (DWT), Fast Fourier Transformation (FFT).
Physiological features	Time-domain features, frequency domain features, Heuristic features, Heart Rate (HR), Heart Rate Variability (HRV), Breathing rate (BR), Dynamic Time Warping (DTW) comparison.
Feature selection algorithms	Principal Component Analysis (PCA), Gradient Descent Boosting (GDB), Support Vector Regression (SVR), k-means clustering, Bayesian Ridge Regression (BRR).
Evaluation metrics	Standard Deviation (SD), Normalised Root Mean Square Error (NRMSE), Mean Absolute Error (MAE), CC Pearson correlation coefficient, Accuracy, `F_1` scores, recall.

3.3 State of the Art

Currently, different wearable sensors are used to estimate physiological features from heart rate and breathing rate. Our focus is to use wrist-worn sensors such as PPG, accelerometer, and gyroscope to extract bio-medical data and use this data to calculate physiological features, and further validate referenced data with a standardised featured dataset. The primary paths to estimate heart rate and breathing rate are shown in the Figure 5.2. Initially, the wrist-worn sensor signal is pre-processed with sampling filters to remove the signal shifts and trends. Further, the peaks are enhanced, and then by using the peaks list, the heart rate is estimated. Breathing rate estimation also follows the same pre-processing methodology.

During the last decade, numerous methodologies are proposed to estimate heart rate and breathing rate parameters from adults to increase their life span and have an active lifestyle.

- Vertens Johand and Fischer et al. (2015) [36] proposed a method to measure respiratory rate and heart rate using a 3D accelerometer and quantify the performance of the system. Three different situations are used to estimate the parameters such as office work, walking, and running on a treadmill. In the pre-processing step, the adaptive low band-pass filter is applied to reduce noise drastically from the time-series signal. Later, heart rate and respiratory rate features are extracted and validated with a standard featured dataset obtained from CPX system (Oxycon Pro-Care Fusion, San Diego CA, USA) for respiratory rate and Polar H7 heart rate belt for heart rate. For validation, Normalised Root Mean Square Error (NRMSE) method and Mean Percentage Error (MPE) is the error calculation method used.

- Wei-jheng et al. (2016) [37] In this paper, a method was proposed to extract physiological information from the photoplethysmography (PPG) sensor signal. In the pre-processing phase, discrete wavelet transforms (DWT) based de-noising filter is applied before artefacts detection and removal. Also, the Kalman filter is proposed to remove unnecessary frequencies. Through this, the Standard Deviation (SD) of peak-to-peak amplitude, Mean Absolute Deviation (MAD) features are extracted. The Support Vector Machines (SVM) algorithm is selected as motion artefacts predictor where the model is optimised with ten-fold cross-validation. Finally, the DWT based features are compared with Kalman filtered features error corrections.

- R.varatharajan et al. (2017) [21] proposed a foot movement monitoring system which is used to detect the onset of a chronic disorder at an early stage. A 3-D accelerometer is used to collect the data from two people aged above 80 years effected with disease and other ten people with a normal health condition. In this paper, dynamic time warping (DTW) algorithm is applied to compare various foot movements collected from the wearable sensor. The foot patterns of healthy individuals and diagnosed patients are separated using mid-level cross identifica-

tion function. The recognised cross levels are used to classify gait signal from the patient. The DTW algorithm classified data compared with various classification algorithms such as inertial navigation algorithm (INA), K-nearest neighbour (k-NN) classifier and support vector machines (SVM). The predicted metrics prove the effectiveness of dynamic time warping (DTW) method.

- Huile Xu et al. (2016) [38]In this paper, the non-linear characteristics of the raw signal is estimated using Hilbert-Huang transformation (HHT). The Public dataset PAMAP2 is taken from the University of California, which contains 12 basic activities, three inertial measurement units (IMUs) and one heart rate monitor as a sensor. Each IMU contains two 3-axis micro-electro-mechanical system (MEMS) accelerometers, 3-axis MEMS gyroscope, and one 3-axis magneto-resistive magnetic sensor. From the wearable sensor data, features are extracted using Hilbert-Huang transformation (HHT) method, the extracted multi-features include instantaneous amplitude (IA) and instantaneous frequency (IF) by means of empirical mode decomposition (EMD), as well as instantaneous energy density (IE) and marginal spectrum (MS) derived from Hilbert spectral analysis. Finally, the backpropagation neural networks proposed by Rumelhart and McClelland in 1986 are used to measure the effect of combining multi-features versus single features are investigated based on a scenario of a dependent and independent subjects with performance metrics such as recall-0.9337, precision-0.9417, F-measures-0.9353 and accuracy-0.9377. The experimental results show that HHT has a remarkable performance when the data is processed from a non-linear and stationary signal.

- Guannan Wu et al. (2017) [30] In the last decade, wearable devices are used for the authentication of health issues, but the majority of authentication methods cannot provide complete certification. For this purpose, the two-step authentication method is proposed based on built-in fingertip sensors such as 3D accelerometer, 3D gyroscope and photoplethysmography (PPG). Total forty volunteers (thirty males and ten females) perform three groups of actions; then each sensor data is pre-processed by reducing noise using Chebyshev low-pass filter with a cut-off frequency of 5 HZ and segmented. Further, the peaks are enhanced and by using the distance between the peaks, physiological features are extracted, including time-domain features: Heart rate variability (HRV), mean, RMSSD. Frequency domain features such as breathing rate, high frequency (HF) are also extracted. Discrete Wavelet Transformation (DWT) domain is generally applied for a non-stationary signal; a total of 78 features are extracted from the time-series data. The Dynamic Time warping (DTW) is applied to estimate the similarity between two sequence signals. In the modelling phase, the one-class machine learning algorithms are applied for identity authentication as a second step. In the experimental results, the average accuracy rate is 98.2%, and F1-score is 86.67%, the output results show that the proposed method is practically applicable and feasible.

- Jeyhani et al. (2015) [39] The Heart rate variability (HRV) is a useful feature domain to analyse cardiac motion artefacts. Usually, HRV is extracted from the ECG signal, but there are being replaced with wearable sensors. This paper focuses on the extraction of HRV from the PPG sensor and compares their vectors with the ground truth ECG signal. Nineteen healthy male subjects are participating in the test. Initially, in the pre-processing phase, the FIR band-pass filters with cut-off frequencies 0.5 and 10 HZ are used to reduce noise in the signal and data is segmented. From the segmented data, peaks are enhanced and to have a better resolution with peaks cubic interpolation is applied. Further, from enhanced peak list, HRV parameters are estimated such as Standard deviation for RR intervals SDNN, Root Mean Square error for adjacent R-R intervals RMSSD, Standard deviation against both axes (SD1, SD2) and Percentage of pairs of adjacent RR intervals differing by more than 50 ms (PNN50). Finally, the extracted feature vectors are compared with ECG features, and measure the mean absolute error, In this study, the largest error from PNN50 is 29.89%, and other HRV parameters have error than 6%.

- Olli Lahdenoja et al. (2016) [40] In this paper, inertial movement sensors such as 3-axis accelerometer and 3-axis gyroscope are used to estimate Heart Rate (HR) and Heart rate variability (HRV) from 29 subjects. At the pre-processing stage, the disturbances in the signal are filtered using single-axis (1-AC) autocorrelation and multi-axis autocorrelation (6-AC). Later the data is segmented and then from each segment, the time and frequency domain features are extracted for both auto-correlation using Kubios software. In the post-processing phase, the inertial features of both types are compared with standard Electrocardiogram (ECG) features and the mean absolute error. The experimental results show that inertial sensors are capable of replacing ECG sensor.

- Hayato Fukushima et al. (2012) [19] Here wrist-type sensor consists of photoplethysmography (PPG) and 3-axis accelerometer is replaced with ECG sensor and collected data in three cases: Resting, Running and Warming-up (aperiodic) on five subjects, In this paper to increase the estimation accuracy of Heart Rate (HR) the accelerometer sensor is added to PPG sensor. In the pre-processing stage, the unwanted motion artifacts are removed. In the case of running, the power spectrum difference between PPG and accelerometer is obtained to remove movement artifacts from the PPG sensor. In the case of warming up, the signal has an aperiodic rate; therefore, by using accelerometer data, the reliability of heart rate is estimated. Further smoothing filters are used to reduce the noise in the data and get segmented, later in frequency analysis. The heart rate is extracted and then compared with standard ECG data, where this device is placed on the torso of a body during the experiment tasks. The experimental results show that the wrist type running case came closer to ECG with high accuracy ($r = 0.98$) and standard deviation (SD =8.7 bpm).

- Adrian Derungs et al. (2018) [41] This paper proposed mistake-drive skill estimation for Nordic walking using the 3D accelerometer, 3D gyroscope and 3D magnetometer, and the data is collected from 10 Nordic walking beginners, the three health risk mistakes are estimated: Matching gear (MS1), Pole use (MS2) and Arm swing (MS3). After reducing noise the strides were used to segment data by using hill climb algorithm, further 351 times, frequency and spectrum domain features are extracted and two feature selection methods such as principal component analysis (PCA), Gradient Descent Boosting (GDB) are applied, from extracted features the skill is estimated by implementing regression-based models Bayesian Ridge Regression (BRR), support vector regression (SVR) evaluation methodology included a leave-one-participant-out (LOPO) cross-validation (CV) across strides. The regression-based skill estimation performance is evaluated by computing standard error calculation metrics such as root-mean-square-error (RMSE), normalised RMSE (nRMSE), and the mean-absolute-error (MAE), from the results it is observed that mistakes can be estimated with RMSE of 24.5% across all participants, An additional trend analysis is performed to improve skill in training sessions.

In Table 3.2, the research papers that are studied and their essential aspects such as the devices used, availability of datasets, physiological features extracted during the research are enumerated. It is important to understand the current methods of research being followed in this field.

Table 3.2: This table summaries important aspects of reviewed research papers.

Paper	Sensor Types	Physiological features	Keys aspects	Dataset availability
[36]	3-D Accelerometer, Heart rate sensor, cpx system, polar H7 heart rate .	Heart rate and Breathing rate	The extracted features are validated with standard featured dataset obtained from CPX system and from heart rate belt.	×
[37]	Photoplethysmography (PPG)	peak-to-peak amplitudes, mean absolute deviation of peak-to-peak amplitudes, the standard deviation of peak-to-peak intervals, and kurtosis Features.	The discrete wavelet transformation features are compared with Kalman filtered features.	×
[21]	3-axis Accelerometer	The Dynamic time warping (DTW) algorithm is applied to compare differently featured pattern.	When DTW algorithm classification results are compared with K-NN, SVM classification algorithms, the DTW has performed better.	×

Paper	Sensor Types	Physiological features	Keys aspects	Dataset availability
[38]	Three Inertial measurement units (IMUs) and one heart rate monitor Each IMU contains two 3-D Accelerometer, 3-D Gyroscope, 3-D Magneto-resistive magnetic sensor.	Instantaneous amplitude (IA), Instantaneous frequency (IF), Instantaneous energy density (IE) and Marginal spectrum (MS), derived from Hilbert spectral analysis.	Based on performance metrics the Hilbert-Huang Transform methodology has remarkable performance while handling the non-linear or non-stationary signals	✓
[30]	3-D Accelerometer, 3-D Gyroscope, and photoplethysmography (PPG) sensor.	Total 78 features are extracted from Time domain: Heart rate Variability features, frequency domain: breathing rate features and Discrete wavelet features.	The DTW is applied to verify sequence patterns, the output results show that the proposed method is practically applicable and feasible	✓
[39]	Photoplethysmograph (PPG) & Electrocardiography (ECG)	Time domain HRV features: SDNN, RMSSD, PNN50, SD_1, SD_2.	The PPG HRV features are compared with ECG ground truth HRV features, for most of the features the MAE is less than 6%	×
[40]	3-D Accelerometer, 3-D Gyroscope, Electrocardiography (ECG)	PPG and ECG Time domain HRV features and Frequency domain BR rate features are extracted using Kubios software and Pan-Tompkins approach	The noise in the signal is filtered using single-axis (1-AC) autocorrelation and multi-axis autocorrelation. The inertial features are compared with standard ECG features	×

Paper	Sensor Types	Physiological features	Keys aspects	Dataset availability
[19]	3-D Accelerometer, Photoplethysmograph (PPG), Electrocardiography (ECG)	Heart rate	The power spectrum difference is calculated between accelerometer signal and ppg signal to remove movement artifacts from PPG signal, The wearable sensors heart rate feature compared with standard ECG data	×
[41]	IMU's (3-D Accelerometer, 3-D Gyroscope, 3-D magnetometer)	Extracted features included: min, max, mean, standard deviation, energy, percentiles, skew, min-max-position of peak, and zero-crossing, total 351 features are extracted.for IMU	Used hill-climb algorithm for data segmentation. The regression based skill estimation between classified features using standard error calculation metrics	×

From the literature review, the research paper presented by Javier Hernandez et al. (2015) is followed to replicate our study. In this paper, the heart rate and breathing rate is estimated from wrist movements. The wrist movements are captured using Samsung galaxy gear smartwatch. This device has 3-axis accelerometer and 3-axis gyroscope sensors, and the experimental data is collected from 12 participants in three different positions (standing up, sitting down, and lying down) in a controlled laboratory environment.

In data preprocessing phase, data is normalized with z-scores, the signal shifts and trends are removed using moving average filter, later the pulse wave and respiratory wave is estimated based on band-pass Butterworth filter cut-off frequencies, from the extracted pulse and respiratory waves the heart rate and breathing rate parameters are evaluated. Further, the experimental features are compared with features set from ECG device and wearable light-based BVP sensor (Empatica E4), while the ground truth data is monitored on three individuals during two consecutive nights of in-situ sleep measurement and followed the above data preprocessing processor mentioned in the paper.

In the evaluation phase, the standard regression-based error calculation methods such as Mean absolute error (MAE), Standard deviation of absolute error (STD), Root Mean Squared Error (RMSE), Person's correlation coefficient (CC) are implemented. However, based on error values, we can say that the accelerometers have outperformed the gyroscope while estimating heart rate and breathing rate, it is vice-versa. However, overall, the BVP measurements are better than motion sensors.

4 Data preprocessing and features extraction

In this chapter, initially, different datasets that are implemented in this project are discussed, and the signal preprocessing process with noise-reducing filters is discussed. In the data preprocessing phase, the pulse wave and the respiratory wave is calculated based on Butterworth filter cut-off frequencies to estimate Heart rate (HR) and Breathing rate (BR) physiological features.

4.1 Data acquisition

In this work, we have considered two different estimating and validating datasets. The first one is sleep recognition dataset and second one is experimentally collected dataset with three different daily life activities. The main intention of data acquisition is to predict the heart rate and breathing rate physiological parameters from the estimating dataset. The estimated features are compared with the validation dataset. The overview of two datasets is explained in below sub-sections.

4.1.1 Sleep recognition data

The sleep recognition data is collected from old aged people wearing wrist-worn device (consists of a 3-D accelerometer, photoplethysmograph (PPG)) and ECG device during their night sleep. The data is recorded for around 9 hours for two different nights of sleep with the ECG device, which has a sampling rate of 100 HZ. The data from the ECG device is already featured as heart rate, and breathing rate physiological parameters, this data can be used for cross-validating the estimated data features. On the other hand, the wrist-worn device data (estimation data) is given as raw signals of PPG, 3-axis accelerometer data with Unix timestamp. This wrist motion data is recorded for 17 minutes during the middle of each night with a sampling rate of 100 HZ, and it is used to estimate heart and breathing rate features from it.

4.1.2 Experimental Dataset

In order to estimate the performance of heart rate and breathing rate features algorithms, experimental tests are performed on two people (one male and one female) with

Empatica E4 wrist wearable device, the device consists of 3-axis accelerometer, photoplethysmograph (PPG), EDA Sensor. While the PPG sensor has a sampling rate of 64 HZ and 3-axis accelerometer has a sampling of 32 HZ. Two minutes recordings were taken with the participant in three positions: resting, walking, sitting. At the end of each session, one-minute rest is provided. From this extracted data, the heart rate and breathing rate physiological features are estimated. Subsequently, the estimated features are cross-validated with ground truth heart Rate and breathing rate features. The ground truth data is taken from the E4 watch application.

4.2 Signal Preprocessing

The signal preprocessing process is implemented to recover the pulse wave and respiratory wave from the raw photoplethysmograph (PPG) and 3-axis accelerometer data signals. Therefore, by using these waveforms the heart rate and breathing rate parameters can be calculated. This methodology is replicated from the referred research paper. The flowcharts 4.1 and 4.3 explains the overview of a PPG signal and 3-axis accelerometer signal preprocessing until the extraction of pulse and respiratory wave.

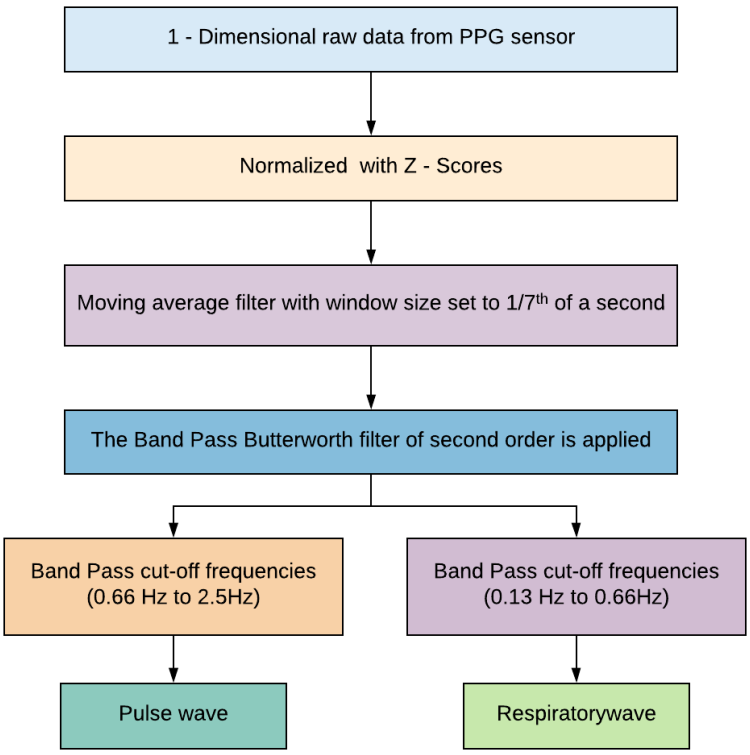

Figure 4.1: The flowchart provides overview of PPG raw data-preprocessing processor till extraction of pulse wave and respiratory wave.

In order to extract heart rate and breathing rate parameters from the wearable sensors data, we have recovered pulse wave and respiratory wave from the raw PPG and accelerometer signals. The below sub-sections explain how both pulse and respiratory waves are estimated. Before estimating both the waveforms, each component of the sensor signal (e.g., X, Y, Z-axis) for accelerometer should be normalized with Z-scores in order to have standard relevance.

4.2.1 Estimation of Pulse Wave

To estimate pulse wave from the 3-axis (e.g., X, Y, Z) accelerometer signal as shown in Figures 4.3. Initially, the Moving Average Filter (MAF) is applied to remove random noise from the data with a set window size of $1/7th$ of a second. Later, bandpass Butterworth filter of order two is applied with low and high bandpass cut off frequencies of 4 and 11 HZ to remove uneven shifts and trends in the data. In order to have a robust estimation, the magnitude is calculated along three components of accelerometer. In the final phase of pulse wave extraction, once again the bandpass Butterworth filter with cut off frequencies 0.66 and 2.5 HZ, which corresponding to 40 and 150 Beats per minute is applied. On the other hand, photoplethysmograph (PPG) have almost followed the similar preprocessing procedure of accelerometer as shown in Figure 4.1, but in case of the PPG sensor, the first bandpass Butterworth filter with cut-off frequencies (4 Hz to 11 Hz) is excluded, and the magnitude of the sensor component is also not calculated because the PPG sensor has a single time axis.

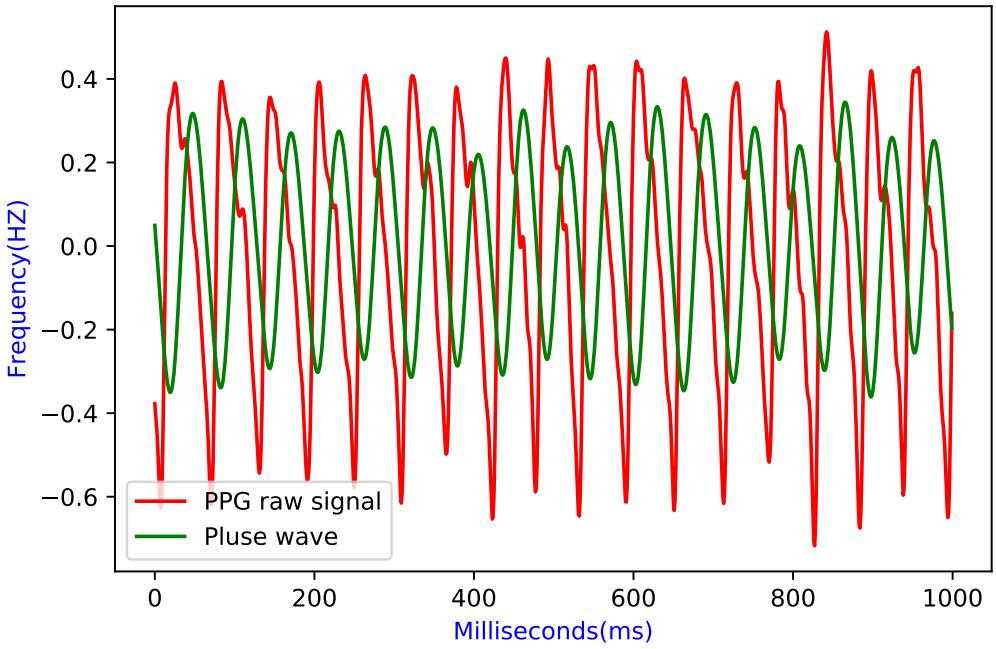

Figure 4.2: An example of raw PPG wave and pulse wave comparison plot

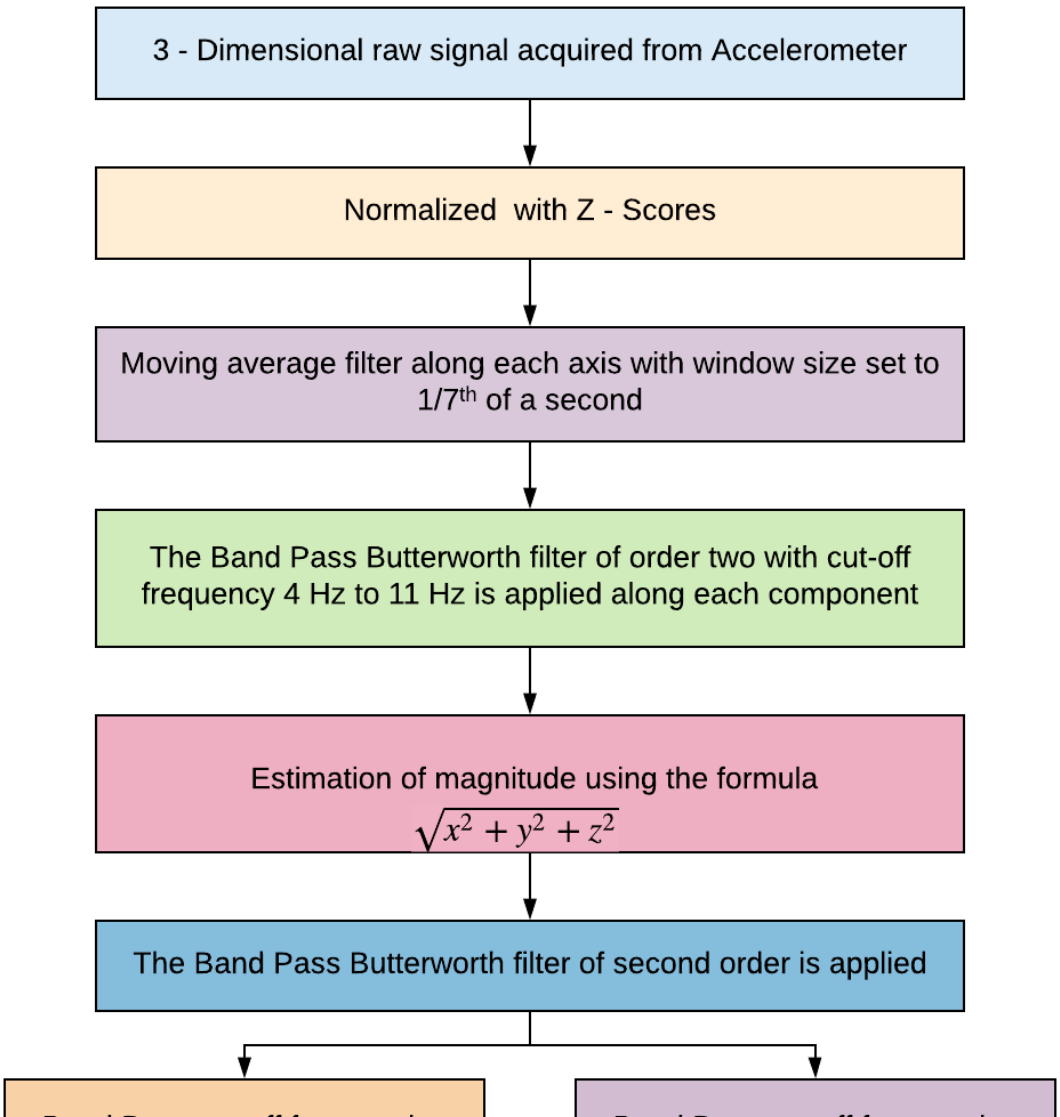

4.2.2 Estimation of Respiratory Wave

The pre-processing method to obtain the respiratory wave pattern from the accelerometer as shown in Figure 4.4 and PPG sensors is similar to the method used to obtain the pulse wave as shown in Figures 4.1, 4.3. The difference being, at the final phase of respiratory wave extraction the band-pass Butterworth filter cut off frequencies are varied with 0.13 and 0.66 (corresponds to 8 and 40 breaths per minute) to remove all pulse or cardiac motions and outputs the periodic signal. Mainly, this respiratory cut off window size is taken empirically as a duration of a respiratory cycle at pre-defined maximum breathing of 40 breaths per minute. In the following two chapters, the heart rate and breathing rate parameters are estimated using pulse and respiratory sinusoidal waveforms.

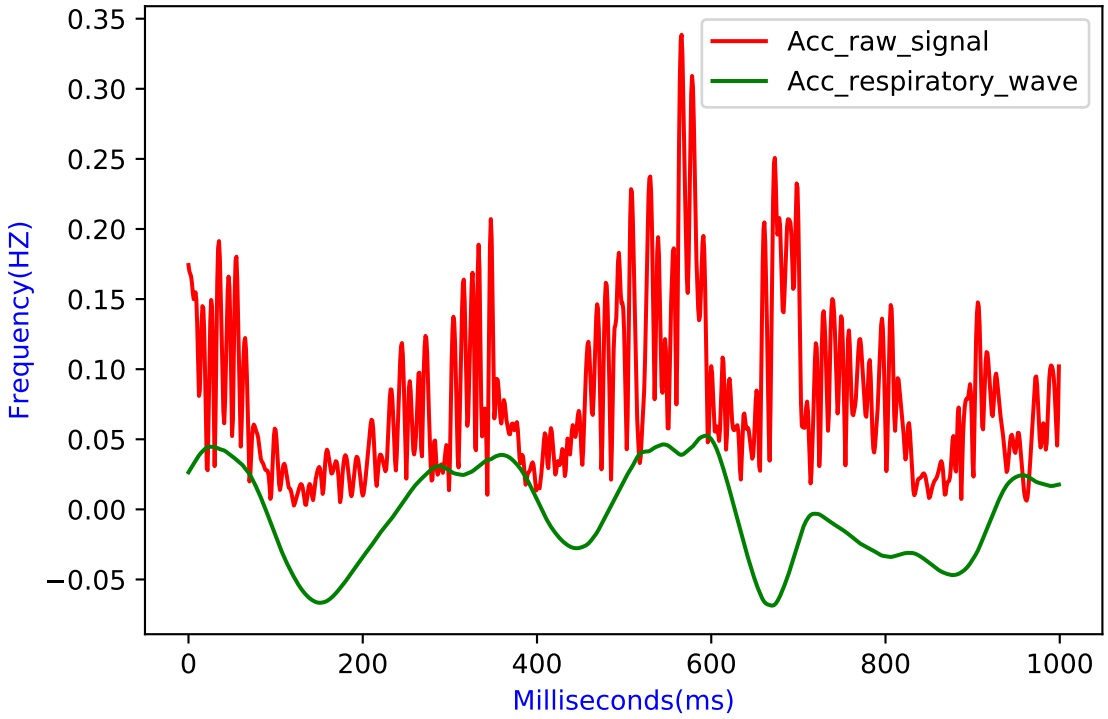

Figure 4.4: An example of raw accelerometer wave and respiratory wave comparison.

5 Heart Rate and Breathing Rate Estimation

This chapter explains the heart rate and breathing rate algorithms, through which the Heart Rate (HR) and Breathing rate (BR) features are extracted from the pulse and respiratory waves from both accelerometer and PPG sensor. Before sending raw time data into the algorithms, both waves are segmented into windows of size (fs*5 sec), fs is the sampling rate of a sensor data per second.

5.1 Pulse Wave Peak Detection

Generally, the heart rate signal consists of beats, where each beat is identified as the Q-R-S complex shown in Figure 5.1 below.

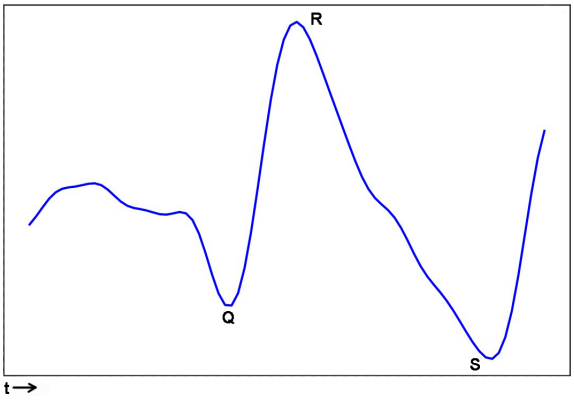

Figure 5.1: Figure shows QRS complex of PPG wave.

In the QRS complex waveform, the initial deflection of the heart rate signal, which is below the baseline is known as Q-wave. The increase in signal with positive deflection is called the R-wave, where R-peaks can be enhanced. The decrease in waveform towards negative deflection is called as S-wave.

The segmented pulse wave dataset is passed into the heart rate algorithm to enhance R-peaks. Firstly, the moving average is calculated for each segment with a window size of 1/7th second, then moving average data is raised by 20% to secure secondary heart rate contractions. Then the local mean is calculated for each segment, and this mean

value compared with each data point in the segmented interval. If the data point is higher than the local mean, it is marked as the region of interest. Out of all the region of interests, the highest value in the window is added to the peak list. The predicted beat positions are appended as R-peak list. If the data point is below the local mean, then the data point is discarded.

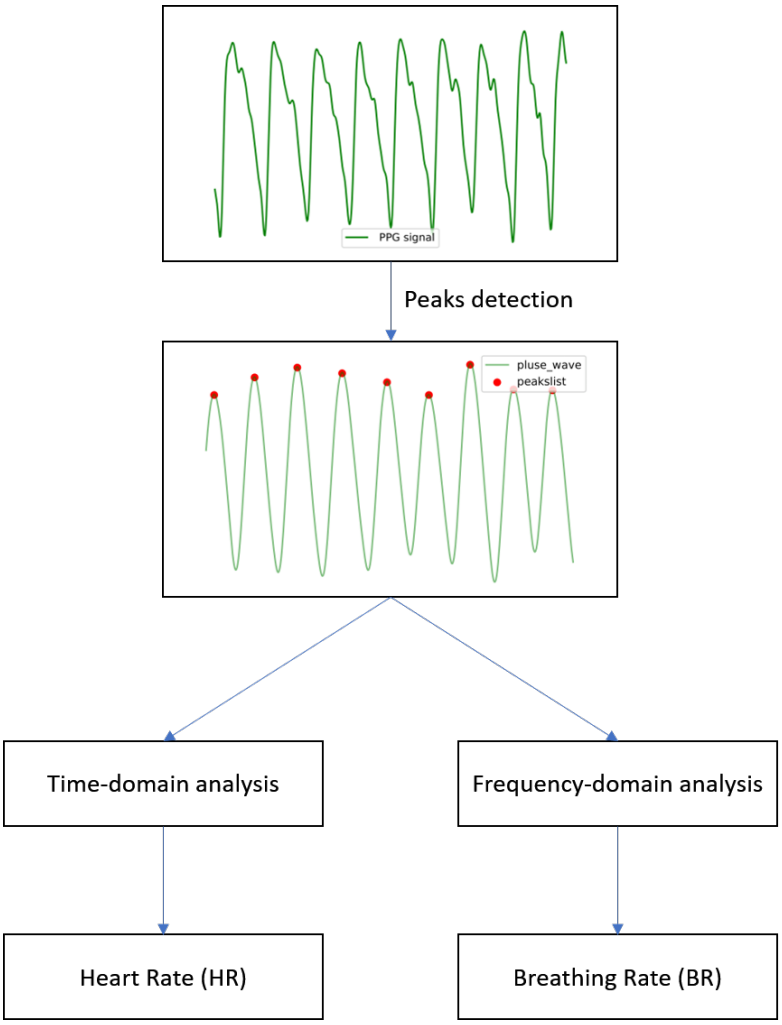

Figure 5.2: The flow chart provides overview of how Heart rate and Breathing rate features are extracted.

5.1.1 Time-domain analysis

Time domain analysis is a measure of time-series variability between successive heartbeats shown. Initially, from the detected regional peaks $R - peaks., R_1, R_2....R_n$the intervals between them $RR_1, RR_2, ...RR_n$ are calculated. The beat difference is indexed

as $R_(i+1) - R_i$, and on the other hand, we should also measure variations between successive instantaneous heart rate intervals (RRvar-1, RRvar-2, RRvarvar-n). Features such as Inter Beat Interval (IBI) and Beats Per Minute (BPM) are described in the below sections [42].

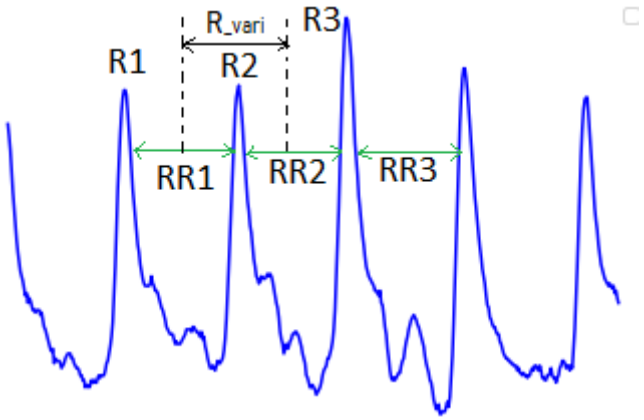

Figure 5.3: Figure representing varying time-series frequency between (R-R intervals) and adjacent (R-R intervals)

5.1.1.1 Inter Beat Interval (IBI)

The mean value of the RR_list is calculated to get the mean Inter Beat Interval (IBI).

$$IBI = np.mean(RR_list) \tag{5.1}$$

5.1.1.2 Beats Per Minute (BPM)

Here, after detecting peaks from time-variable heart rate signal, the distance between the peaks is calculate and averaged and is converted into beats per minute value.

$$BPM = \frac{6000}{mean(\overline{RR}_(list))} \tag{5.2}$$

5.2 Breathing Rate Estimation

The segmented respiratory wave is passed into the breathing rate algorithm, and the breathing rate feature is estimated in the frequency domain analysis. This breathing rate algorithm is similar to the heart rate algorithm until the estimation of peak lists and appended R-R interval list. Then, to estimate the breathing rate in the frequency domain, we have created an equally spaced timeline for each RR_list by referring to the

beat positions of R-peaks. The timeline signal is interpolated using the cubic spline interpolation to increase the generality between varying R-R intervals. Later, this interpolated R-R signal is passed into Fast Fourier transformation (FFT) to extract frequency wave. In the below subsection, the theoretical overview of frequency domain analysis is given with an example plot.

5.2.1 Frequency-domain analysis

In order to convert time-domain analysis into frequency domain analysis the Fast Fourier transformation is applied. The Fourier transformation is applicable for evenly spaced or distributed data. However, in this work, the distance between R-R peaks is uneven with respect to time. Researchers suggest the interpolation of the frequency signal, the interpolation of the signal is also known as a re-sampling method. Then the transformed time-frequency data using Fourier transformation is mapped into frequency domain as shown in the below Figure 5.4 [31].

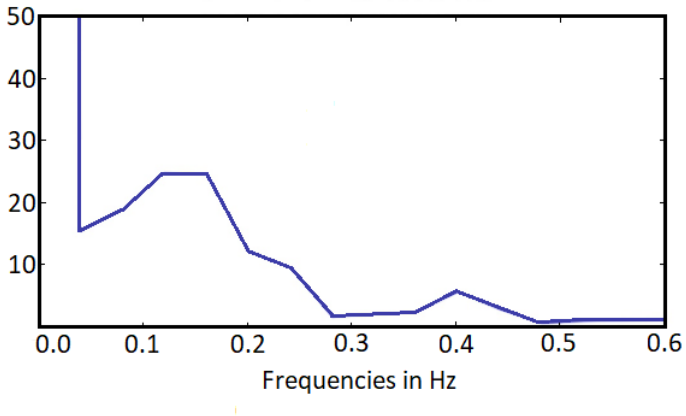

Figure 5.4: Frequency spectrum of Heart Rate Variability [7]

In frequency domain analysis, the breathing-rate signal is divided into LF (Low Frequency), MF (Mid Frequency), and HF (High Frequency). However, the MF and HF together are labelled as HF. The frequency band of LF is (0.04-0.15 Hz), and it relates to short-term blood pressure variation. On the other hand frequency range of HF with (0.16-0.5 Hz), HF indicates the breathing rate estimation signal [7] [43].

5.2.2 Breathing rate (BR) feature

In Breathing Rate (BR) estimation algorithm, once again, the peaks are enhanced from the extracted frequency signal, the procedure followed is similar to the peaks detection procedure of heart rate algorithm given above. In the final phase of breathing rate

algorithm, the segmented peaks list from the frequency wave and the length of the original respiratory wave is used. The breathing formula for signal segmented window can be represented as:

$$signal\ time = \frac{len(Respiratory\ signal)}{Sampling\ rate} \tag{5.3}$$

$$Breathing\ rate = \frac{len(frequency\ wave\ peakslist)}{signal\ time} \tag{5.4}$$

6 Results and Discussions

In this work, the physiological features such as: heart rate and breathing rate from sleep recognition and Empatica E4 datasets have been estimated, the details about them are explained in subsections 4.1.1 & 4.1.2. In order to understand the feasibility of the estimated features, we have validated them with ground truth featured datasets. The estimated features from sleep recognition dataset are cross-validated with the heart rate and breathing rate features taken by ECG. The features estimated from the raw data of the Empatica E4 dataset are compared with E4 watch application data which gives heart rate and Inter Beat Interval (IBI). To evaluate the difference between the estimated and ground-truth features, standard error calculation methods such as mean absolute error (MAE), mean squared error (MSE) and correlations coefficient (CC) is utilised.

Heart rate validation for Sleep recognition data

In this section, the heart rate extracted from the sleep recognition dataset of two subjects taken using the PPG and accelerometer sensor is cross-validated with the ground truth feature taken from the ECG device.

Table 6.1: Error metrics of Heart Rate for sleep recognition data

Sensor	Subject	RMSE	MAE	CC
PPG	1	20.093	14.577	0.077
Accelerometer	1	69.004	59.064	0.1728
PPG	2	23.673	18.891	0.1022
Accelerometer	2	61.287	47.205	-0.010

The standard evaluation metrics such as Root Mean Square Error (RMSE), Mean Absolute Error (MAE) and Correlation coefficient (CC) are calculated by using the estimated heart rate, and ground truth heart rate featured datasets. By looking at the Table 6.1, It is clear that the estimated heart rate feature of PPG sensor has outperformed the accelerometer heart rate feature for both the subjects. It can be observed that RMSE

and MAE error values in the accelerometer are three times the error produced in the PPG sensor. Also, in case of Pearson correlation coefficient, the values are better for the PPG sensor when compared to the accelerometer.

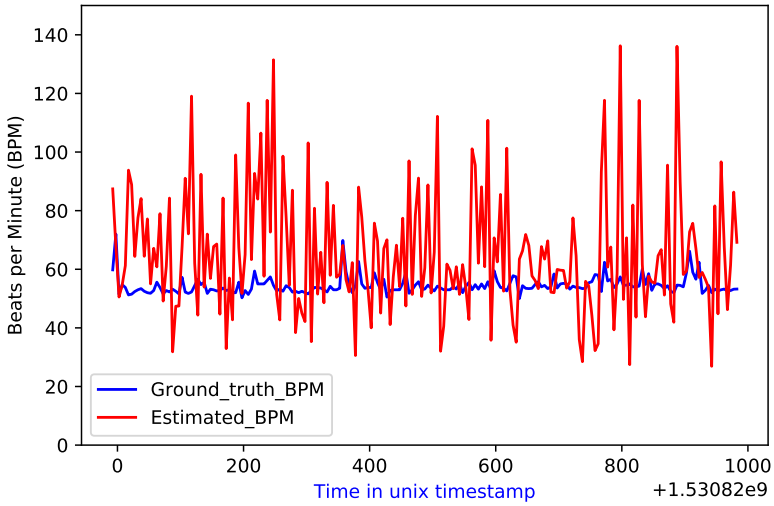

Figure 6.1: The plot shows the comparison of estimated and ground truth heart rate feature for sleep recognition PPG sensor data set, for subject-1.

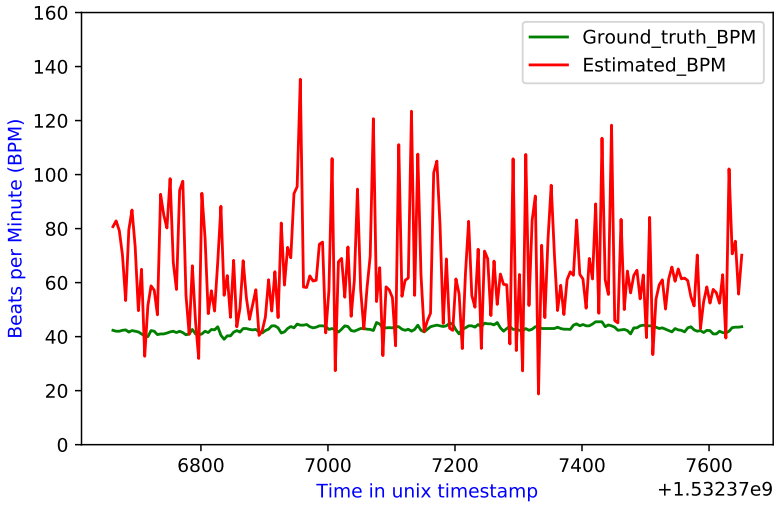

Figure 6.2: The plot shows the comparison of estimated and ground truth heart rate feature for sleep recognition PPG data set, for subject subject-2.

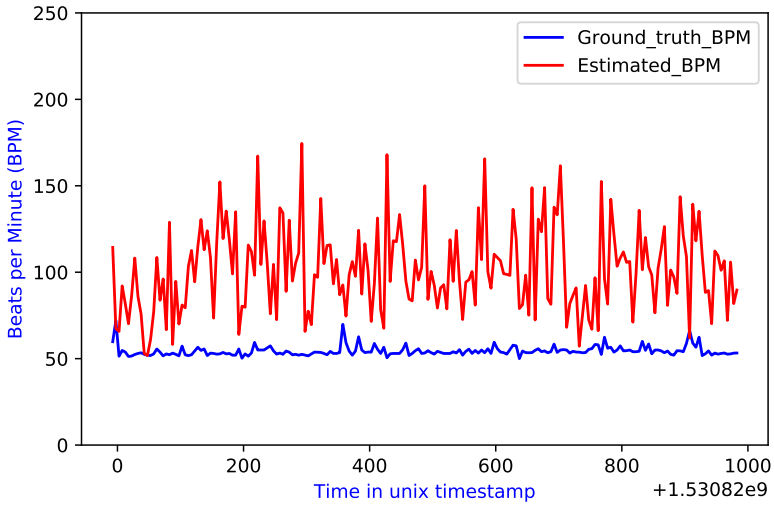

Figure 6.3: The plot shows the comparison of estimated and ground truth heart rate feature for sleep recognition 3-axis accelerometer data set, for subject-1.

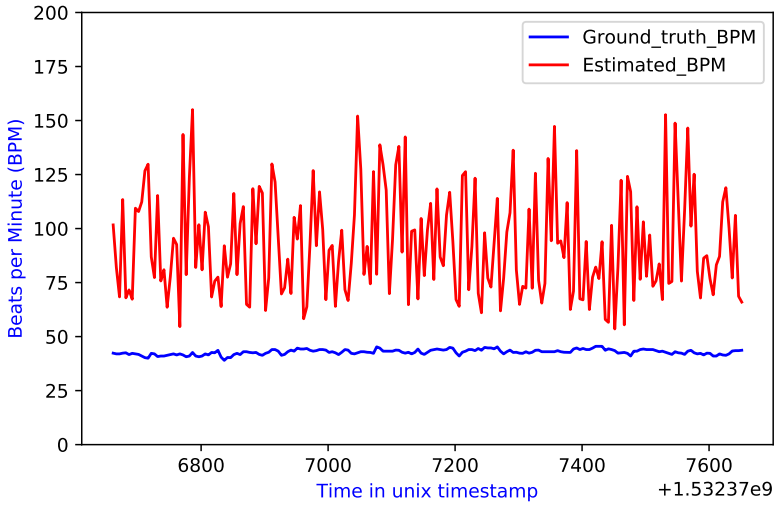

Figure 6.4: The plot shows the comparison of estimated and ground truth heart rate feature for sleep recognition 3-axis accelerometer data set, for subject-2.

From the above heart rate comparison (Figures 6.1 to 6.4), it is observed that the estimated PPG heart rate feature is more comparable to the ground truth than the accelerometer heart rate feature for both the subjects.

Heart rate and IBI validation for Empatica E4 data

Here, we have validated the estimated Heart rate (HR) and Inter Beat Interval (IBI) features taken using a PPG sensor with ground truth heart rate and IBI features taken from E4 watch application.

Table 6.2: Error metrics of Heart Rate and IBI features for Empatica E4 data

Sensor	Subject	RMSE	MAE	CC
PPG Heart Rate	1	22.475	17.359	0.011
PPG IBI	1	1.215	1.035	0.072
PPG Heart Rate	2	23.974	14.870	0.024
PPG IBI	2	0.5511	0.531	-0.047

The above Table 6.2 shows evaluated error metrics. The evaluation is done between the estimated Empatica E4 PPG sensor's heart rate, IBI features and the ground truth heart rate and IBI features taken from the watch application. The RMSE values for the PPG heart rate of the two subjects are almost similar, but the Mean absolute error and correction coefficient values vary by 3%. Based on these evaluated error metrics, we can say that the estimated heart rate feature of Empahtica E4 PPG sensor is comparable with ground truth heart rate feature. The subject-1 has positive correction coefficient (CC:0.0721) and subject-2 has negative correction coefficient (CC:-0.047). The negative correction value implies the increase in estimated IBI values and decrease in ground truth IBI values.

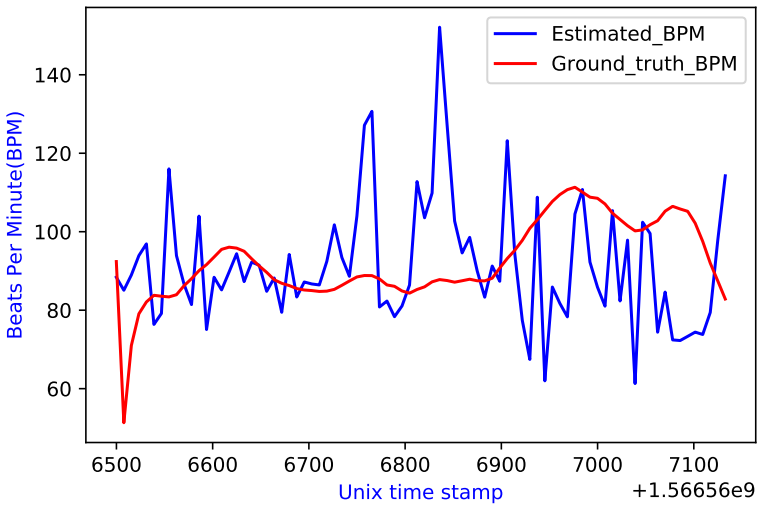

Figure 6.5: The plot shows the comparison of estimated and ground truth heart rate feature for Empatica E4 PPG data set, for subject-1.

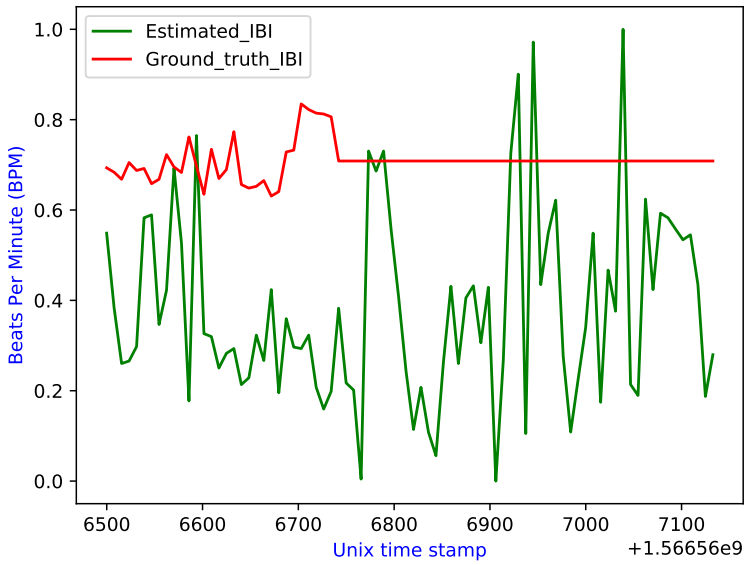

Figure 6.6: The plot shows the comparison of estimated and ground truth IBI feature for Empatica E4 PPG data set, for subject-1.

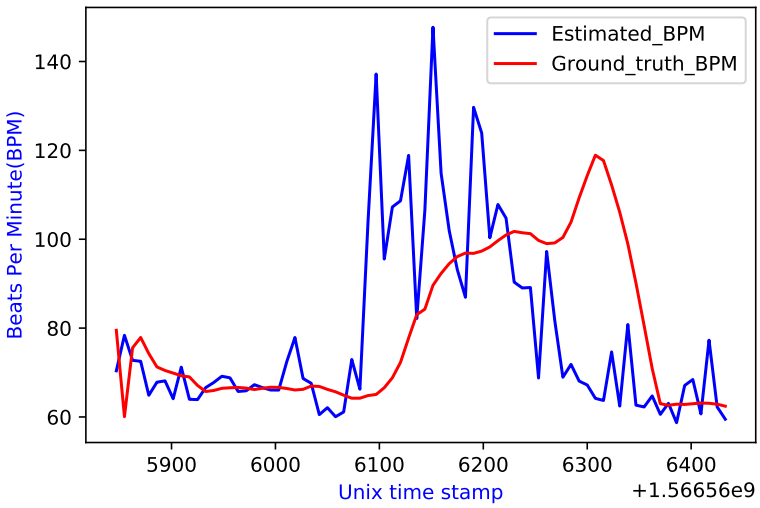

Figure 6.7: The plot shows the comparison of estimated and ground truth heart rate feature for Empatica E4 PPG data set, for subject-2.

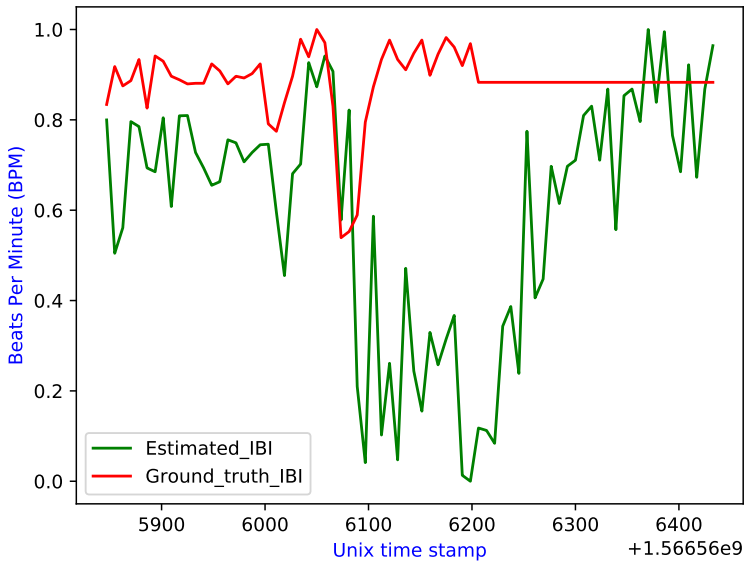

Figure 6.8: The plot shows the comparison of estimated and ground truth IBI feature for Empatica E4 PPG data set, for subject-2.

By looking at these figures (6.5 and 6.7) we can say that the both subjects' estimated heart rate feature has marginally followed the trend of ground truth heart rate feature.

Breathing rate validation for the sleep recognition data

This section describes the error metrics for the estimated breathing rate feature taken from the accelerometer and ECG ground truth breathing rate. At the same time, we have excluded the calculation of breathing rate error metrics and comparison plots for the sleep recognition data taken from the PPG sensor. The breathing rate error metrics have been excluded because most of the predicted peaks are less than four for each segmented window size, and this length does not fit into the cubical spline interpolation method. Therefore, no breathing curve is obtained to estimate the breathing rate feature. This non-response might be due to abnormal fluctuations in the sign

Table 6.3: Error metrics of breathing rate for sleep recognition data

Sensor	Subject	RMSE	MAE	CC
Accelerometer	1	6.288	4.980	0.158
Accelerometer	2	3.765	3.114	0.2049

Table 6.3 shows the breathing rate evaluation metrics for 3-axis accelerometer. The root mean square error (RMSE: 3.765) and mean absolute error (MAE:0.2049) values of subject-2 is less than the subject-1, even it has better correction coefficient (CC:0.2049). The breathing rate comparison Figures 6.9, 6.10 for two subjects, indicates that the accelerometer breathing rate feature has feasibility with ground truth ECG sensor breathing rate feature. The estimated breathing rate Figure 6.10 of subject-2 has better ground truth comparison trend than the subject-1 as shown in Figure 6.9.

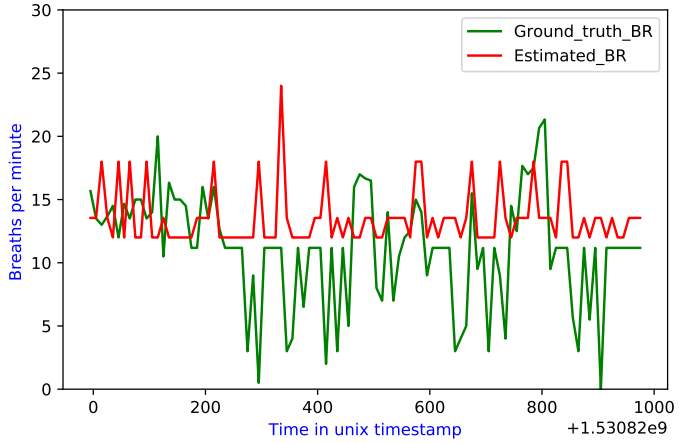

Figure 6.9: The plot shows the comparison of estimated and ground truth Breathing rate feature for sleep recognition accelerometer data set, for subject-1.

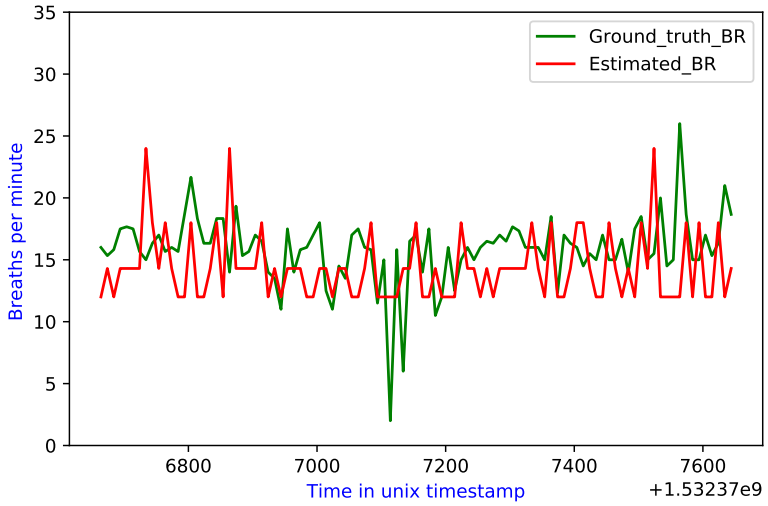

Figure 6.10: The plot shows the comparison of estimated and ground truth Breathing rate feature for sleep recognition accelerometer data set, for subject-1.

Breathing rate estimation for Empatica E4 data

Here, we have only plotted the two subjects estimated breathing rate feature for the Empatica E4 PPG and 3-axis accelerometer signal and excluded the calculation of Root Mean Square Error (RMSE), Mean Absolute Error (MAE), Correlation Coefficient (CC) values, because the Empatica E4 wristwatch does not provide the ground truth for breathing rate feature set.

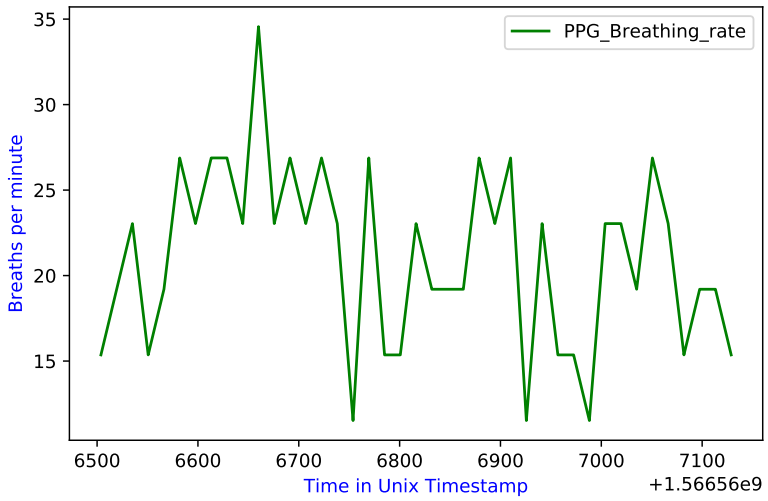

Figure 6.11: The plot shows estimated breathing rate parameters, extracted from E4 PPG data set, for subject-1.

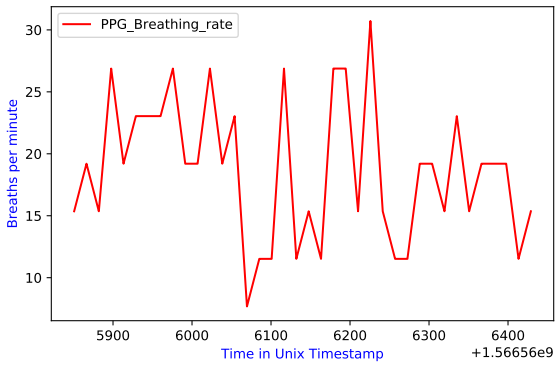

Figure 6.12: The plot shows estimated breathing rate parameters, extracted from E4 PPG data set, for subject-2

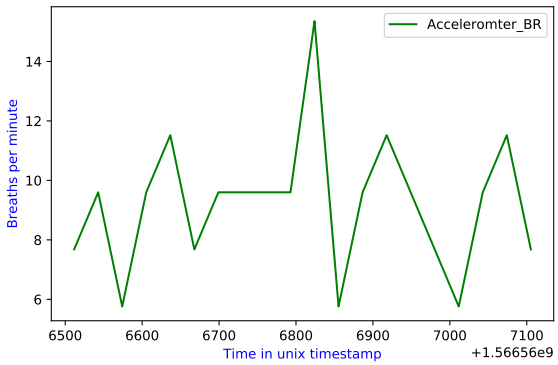

Figure 6.13: The plot shows estimated breathing rate parameters, extracted from E4 accelerometer data set, for subject-1.

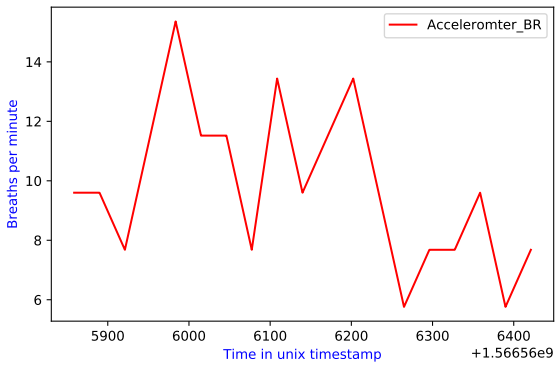

Figure 6.14: The plot shows estimated breathing rate parameters, extracted from E4 accelerometer data set, for subject-2.

7 Conclusion and Future work

The main goal of this thesis is to estimate physiological features from the data obtained from wristwatch sensors that have PPG and 3-axis accelerometer sensor. These estimated features are cross-validated with the ground truth features. Our approach is motivated by the previous work performed using a wrist-worn sensor.

In this work, both Heart Rate (HR) estimation and Breathing Rate (BR) estimation algorithms of PPG and accelerometer sensors are developed. These algorithms have followed similar signal pre-processing and post-processing procedure, taken from the reference paper. In order to evaluate heart and breathing rate algorithms, we have considered sleep recognition dataset and Empatica E4 dataset taken from two participants. During the evaluation process, in the signal processing phase, the Heart Rate (HR) feature is extracted from the pulse wave and the Breathing Rate (BR) feature is extracted from the respiratory wave.

The estimated features are cross-validated with ground truth heart rate and breathing rate features. In the post-processing phase, for the sleep recognition data, the heart rate evaluation metrics from the PPG sensor outperformed the accelerometer sensor. On the other hand, the breathing rate evaluation metrics are calculated for only the accelerometer data.

After going through the results, we can conclude that for the calculation of Heart Rate (HR) PPG sensor is preferred over the accelerometer sensor. The error metrics of heart rate estimation from the PPG are similar for both datasets, with an average error of 20 beats per minute. Also, as the error is minimal, the ECG devices can be replaced with the wrist-worn sensors to estimate the physiological features such as heart rates and breathing rates.

Bibliography

[1] Z. Zhu, T. Liu, G. Li, T. Li, and Y. Inoue, "Wearable sensor systems for infants," *Sensors*, vol. 15, no. 2, pp. 3721–3749, 2015.

[2] S. Goudarzvand, J. S. Sauver, M. M. Mielke, P. Y. Takahashi, Y. Lee, and S. Sohn, "Early temporal characteristics of elderly patient cognitive impairment in electronic health records," *BMC medical informatics and decision making*, vol. 19, no. 4, pp. 1–14, 2019.

[3] A. L. S. De Lima, L. J. Evers, T. Hahn, L. Bataille, J. L. Hamilton, M. A. Little, Y. Okuma, B. R. Bloem, and M. J. Faber, "Freezing of gait and fall detection in parkinson's disease using wearable sensors: a systematic review," *Journal of neurology*, vol. 264, no. 8, pp. 1642–1654, 2017.

[4] A. Sadiq, N. Othman, M. A. Jamil, M. Youseffi, M. Denyer, W. W. Zakaria, and M. M. Tomari, "Fourth-order butterworth active bandpass filter design for single-sided magnetic particle imaging scanner," *Journal of Telecommunication, Electronic and Computer Engineering (JTEC)*, vol. 10, no. 1-17, pp. 17–21, 2018.

[5] "Introduction to analog devices."

[6] B. Khelil, A. Kachouri, M. B. Messaoud, and H. Ghariani, "P wave analysis in ecg signals using correlation for arrhythmias detection," in *4th International multi-conference on systems, signals & devices*, vol. 3, 2007.

[7] L. Lee, R. Campbell, M. Scheuermann-Freestone, R. Taylor, P. Gunaruwan, L. Williams, H. Ashrafian, J. Horowitz, A. G. Fraser, K. Clarke *et al.*, "Metabolic modulation with perhexiline in chronic heart failure: a randomized, controlled trial of short-term use of a novel treatment," *Circulation*, vol. 112, no. 21, pp. 3280–3288, 2005.

[8] P. Lustig, "The cots-threshold," in *Proceedings of Things*, 2005.

[9] A. Alzheimer's, "Alzheimer's disease facts and figures, alzheimer's dement," *J. Alzheimer's Assoc*, vol. 11, no. 3, 2015.

[10] M. Lillo-Crespo, J. Riquelme, R. Macrae, W. De Abreu, E. Hanson, I. Holmerova, M. J. Cabañero, R. Ferrer, and D. Tolson, "Experiences of advanced dementia care in seven european countries: implications for educating the workforce," *Global health action*, vol. 11, no. 1, p. 1478686, 2018.

[11] R. H. Fortinsky and J. H. Wasson, "How do physicians diagnose dementia? evidence from clinical vignette responses," *American Journal of Alzheimer's Disease*, vol. 12, no. 2, pp. 51–61, 1997.

[12] U. Lundberg, R. Kadefors, B. Melin, G. Palmerud, P. Hassmén, M. Engström, and I. E. Dohns, "Psychophysiological stress and emg activity of the trapezius muscle," *International journal of behavioral medicine*, vol. 1, no. 4, pp. 354–370, 1994.

[13] J. Vertens, F. Fischer, C. Heyde, F. Hoeflinger, R. Zhang, L. M. Reindl, and A. Gollhofer, "Measuring respiration and heart rate using two acceleration sensors on a fully embedded platform." in *icSPORTS*, 2015, pp. 15–23.

[14] G. Wu, J. Wang, Y. Zhang, and S. Jiang, "A continuous identity authentication scheme based on physiological and behavioral characteristics," *Sensors*, vol. 18, no. 1, p. 179, 2018.

[15] H. Selye, "The stress syndrome," *The American Journal of Nursing*, pp. 97–99, 1965.

[16] C. C. Poon, Y. M. Wong, and Y.-T. Zhang, "M-health: the development of cuffless and wearable blood pressure meters for use in body sensor networks," in *2006 IEEE/NLM Life Science Systems and Applications Workshop*. IEEE, 2006, pp. 1–2.

[17] Y. Zheng, B. Leung, S. Sy, Y. Zhang, and C. C. Poon, "A clip-free eyeglasses-based wearable monitoring device for measuring photoplethysmograhic signals," in *2012 Annual International Conference of the IEEE Engineering in Medicine and Biology Society*. IEEE, 2012, pp. 5022–5025.

[18] M. Rothmaier, B. Selm, S. Spichtig, D. Haensse, and M. Wolf, "Photonic textiles for pulse oximetry," *Optics express*, vol. 16, no. 17, pp. 12 973–12 986, 2008.

[19] H. Fukushima, H. Kawanaka, M. S. Bhuiyan, and K. Oguri, "Estimating heart rate using wrist-type photoplethysmography and acceleration sensor while running," in *2012 Annual International Conference of the IEEE Engineering in Medicine and Biology Society*. IEEE, 2012, pp. 2901–2904.

[20] L. E. Hebert, P. A. Scherr, J. L. Bienias, D. A. Bennett, and D. A. Evans, "Alzheimer disease in the us population: prevalence estimates using the 2000 census," *Archives of neurology*, vol. 60, no. 8, pp. 1119–1122, 2003.

[21] R. Varatharajan, G. Manogaran, M. K. Priyan, and R. Sundarasekar, "Wearable sensor devices for early detection of alzheimer disease using dynamic time warping algorithm," *Cluster Computing*, vol. 21, no. 1, pp. 681–690, 2018.

[22] H. Zeng and Y. Zhao, "Sensing movement: Microsensors for body motion measurement," *Sensors*, vol. 11, no. 1, pp. 638–660, 2011.

[23] O. Edwards, J. Galley, R. Courtenay-Evans, J. Hunter, and A. Tait, "Changes in cortisol metabolism following rifampicin therapy," *The Lancet*, vol. 304, no. 7880, pp. 549–551, 1974.

[24] J. F. Thayer, F. Åhs, M. Fredrikson, J. J. Sollers III, and T. D. Wager, "A meta-analysis of heart rate variability and neuroimaging studies: implications for heart rate variability as a marker of stress and health," *Neuroscience & Biobehavioral Reviews*, vol. 36, no. 2, pp. 747–756, 2012.

[25] G. K. Jaiswal and R. Paul, "Artificial neural network for ecg classification," *Recent Research in Science and Technology*, 2014.

[26] J. M. Medeiros, "Development of a heart rate variability analysis tool," Master's thesis, 2010.

[27] J. Hernandez, D. McDuff, and R. W. Picard, "Biowatch: estimation of heart and breathing rates from wrist motions," in *2015 9th International Conference on Pervasive Computing Technologies for Healthcare (PervasiveHealth)*. IEEE, 2015, pp. 169–176.

[28] J. Brownlee, "moving-average-smoothing-for-time-series-forecasting-python." Machine Learning Mastery, Dec 28, 2016.

[29] S. W. Smith *et al.*, "The scientist and engineer's guide to digital signal processing," 1997.

[30] G. Wu, J. Wang, Y. Zhang, and S. Jiang, "A continuous identity authentication scheme based on physiological and behavioral characteristics," *Sensors*, vol. 18, no. 1, p. 179, 2018.

[31] M. Boyett and H. Dobrzynski, "The sinoatrial node is still setting the pace 100 years after its discovery," 2007.

[32] G. D. Clifford, F. Azuaje, and P. Mcsharry, "Ecg statistics, noise, artifacts, and missing data," *Advanced methods and tools for ECG data analysis*, vol. 6, p. 18, 2006.

[33] P. Welch, "The use of fast fourier transform for the estimation of power spectra: a method based on time averaging over short, modified periodograms," *IEEE Transactions on audio and electroacoustics*, vol. 15, no. 2, pp. 70–73, 1967.

[34] E. Von Borell, J. Langbein, G. Després, S. Hansen, C. Leterrier, J. Marchant-Forde, R. Marchant-Forde, M. Minero, E. Mohr, A. Prunier *et al.*, "Heart rate variability as a measure of autonomic regulation of cardiac activity for assessing stress and welfare in farm animals—a review," *Physiology & behavior*, vol. 92, no. 3, pp. 293–316, 2007.

[35] C. J. Willmott and K. Matsuura, "Advantages of the mean absolute error (mae) over the root mean square error (rmse) in assessing average model performance," *Climate research*, vol. 30, no. 1, pp. 79–82, 2005.

[36] J. Vertens, F. Fischer, C. Heyde, F. Hoeflinger, R. Zhang, L. M. Reindl, and A. Gollhofer, "Measuring respiration and heart rate using two acceleration sensors on a fully embedded platform." in *icSPORTS*, 2015, pp. 15–23.

[37] W.-J. Lin and H.-P. Ma, "A physiological information extraction method based on wearable ppg sensors with motion artifact removal," in *2016 IEEE International Conference on Communications (ICC)*. IEEE, 2016, pp. 1–6.

[38] H. Xu, J. Liu, H. Hu, and Y. Zhang, "Wearable sensor-based human activity recognition method with multi-features extracted from hilbert-huang transform," *Sensors*, vol. 16, no. 12, p. 2048, 2016.

[39] V. Jeyhani, S. Mahdiani, M. Peltokangas, and A. Vehkaoja, "Comparison of hrv parameters derived from photoplethysmography and electrocardiography signals," in *2015 37th Annual International Conference of the IEEE Engineering in Medicine and Biology Society (EMBC)*. IEEE, 2015, pp. 5952–5955.

[40] O. Lahdenoja, T. Humanen, M. J. Tadi, M. Pänkäälä, and T. Koivisto, "Heart rate variability estimation with joint accelerometer and gyroscope sensing," in *2016 Computing in Cardiology Conference (CinC)*. IEEE, 2016, pp. 717–720.

[41] A. Derungs, S. Soller, A. Weishäupl, J. Bleuel, G. Berschin, and O. Amft, "Regression-based, mistake-driven movement skill estimation in nordic walking using wearable inertial sensors," in *2018 IEEE International Conference on Pervasive Computing and Communications (PerCom)*. IEEE, 2018, pp. 1–10.

[42] F. Al-Shargie, "Early detection of mental stress using advanced neuroimaging and artificial intelligence," *arXiv preprint arXiv:1903.08511*, 2019.

[43] P. van Gent, "Analyzing a discrete heart rate signal using python," *A Tech Blog About Fun Things With Python and Embedded Electronics. http://www. paulvangent. com/2016/03/15/analyzing-a-discrete-heart-rate-signal-using-python-part-1/. Google Scholar*, 2016.

Declaration of work

I declare that this thesis, which I submit to University of Rostock for examination in consideration of the award of a higher degree of "Masters in Science" is my own personal effort. Where any of the content presented is the result of input or data from a related collaborative research programme this is duly acknowledged in the text such that it is possible to ascertain how much of the work is my own. I have not already obtained a degree in a University or elsewhere on the basis of this work. Furthermore, I took reasonable care to ensure that the work is original, and, to the best of my knowledge, does not breach copyright law, and has not been taken from other sources except where such work has been cited and acknowledged within the text.

Rostock,

_____

Manoj Sai Ghanta